CHAPTER

4

Cenozoic tectonic evolution of the North Andes with constraints from volcanic ages, seismic reflection, and satellite geodesy

James N. Kellogg*, Gabriela Beatriz Franco Camelio[†], Héctor Mora-Páez[‡]

University of South Carolina, Columbia, SC, United States Simon Bolivar University, Caracas, Venezuela[†] Colombian Geological Survey, Space Geodesy Research Group, Bogota, Colombia[‡]*

1 Introduction

The Cenozoic evolution of the northern Andes can provide important insights to answer questions about Andean margin processes, such as how slip is partitioned at complex obliquely convergent plate boundaries, how mountain building rates and styles can be correlated with convergent boundary processes, and what are the kinematics of an active arc-continent collision and accretion. We propose in this chapter that buoyant Caribbean crust has been amagmatically subducting under the North Andes for 75 Myr. We also summarize previous work that shows that convergent boundary forces have inverted and shortened a basin up to 150 km forming the Eastern Cordillera mountain range, 6 "US Rocky Mountain Laramide-style" (basement block) mountain ranges have been rapidly uplifted 7–12 km in the last 10 Myr, and several island arcs have collided with the North Andean margin. We also review recent GPS results that show that the Panama arc is actively colliding with the North Andean Block (NAB), having recently formed a land bridge between the Americas, separating the Atlantic and Pacific Oceans (e.g., Freymueller et al., 1993; Mora-Páez et al., 2019). Part of the Panama-Choco arc has recently accreted to the NAB (Kellogg and Mora-Páez, 2016), and the entire block has begun to slide parallel to the continental margin toward the Caribbean (e.g., Ego et al., 1996; Audemard et al., 1999; Tibaldi et al., 2007; Egbue and Kellogg, 2010).

1.1 Flat subduction

Very little attention has been paid to the vast surface area of the flat slab subducted under the northern Andes in the last 80 Myr, including half of the buoyant Caribbean Large Igneous Province (we estimate as approximately $1.8 \times 10^6 km^2$). Approximately 10% of present-day subduction zones are considered to have flat slabs, which means that their dip angle beyond the seismogenic zone is very shallow (Gutscher et al., 2000). This phenomenon has been shown to exist in the geologic record where cycles of alternating flat (rigid basement tectonics, no volcanic arc) and normal-dip subduction are proposed (James and

Andean Tectonics. https://doi.org/10.1016/B978-0-12-816009-1.00006-X

Sacks, 1999; DeCelles et al., 2009; Ramos and Folguera, 2009). Proposed causes for flat-to-shallow subduction include trenchward motion of the upper plate in an absolute plate motion sense, mantle wedge suction (van Hunen et al., 2004), and excess positive buoyancy related to thickened oceanic crust of the subducting plate (Livaccari et al., 1981; Pilger, 1981; Cross and Pilger, 1982; Nur and Ben-Avraham, 1983; Gutscher et al., 1999, 2000; Saleeby, 2003; Anderson et al., 2007; Liu et al., 2010).

1.2 Slab geometry

Wadati-Benioff zone seismicity beneath Colombia is located in two bands, offset by a ~250 km offset at 5°N, which coincides with the northern termination of arc volcanism (Fig. 2, e.g., Pennington, 1981; Ojeda and Havskov, 2001; Vargas and Mann, 2013). The slab north of this offset is often referred to as the Bucaramanga segment, and the southern slab is referred to as the Cauca segment (Pennington, 1981). Within the Bucaramanga segment lies the Bucaramanga nest, a localized region of seismicity containing among the highest concentrations of intermediate-depth seismicity globally (e.g., Prieto et al., 2012). One group of models attributes the Cauca segment to a Nazca origin and the Bucaramanga segment to a Caribbean origin, with the Bucaramanga nest located within the Caribbean plate (Malavé and Suárez, 1995; Taboada et al., 2000; Cortés and Angelier, 2005; Vargas et al., 2007; Prieto et al., 2012; Yarce et al., 2014). In several models, the northern edge of the Cauca segment and the southern edge of the Bucaramanga segment overlap (Taboada et al., 2000; Cortés and Angelier, 2005; Vargas et al., 2007; Vargas and Mann, 2013). Others attribute the ~250 km offset in slab seismicity to a tear in the Nazca slab with the Nazca - Caribbean boundary at the Bucaramanga nest (Corredor, 2003; Zarifi et al., 2007; Sanchez-Rojas and Palma, 2014; Chiarabba et al., 2015; Syracuse et al., 2016). The revised plate motion model presented in this chapter predicts that the flat-subducting paleo-Caribbean slab would be located in the present position of the "Bucaramanga slab" and that the "Caldas tear" is actually the southern edge of the Caribbean plate (see Fig. 7 and Section 5.3).

1.3 Arc-continent accretion and "escape"

From terrane models, it has been shown that continents can grow by the collisional accretion of numerous terranes, large (thousands of square kilometers) and small (1 or 2 km^2) (e.g., Nur and Ben-Avraham, 1983). The Cenozoic history of the western plate interface of the central and southern Andes has been characterized by subduction erosion (e.g., Horton, 2018), while the northern Andean margin has been characterized by continental accretion: plateau-continent collision (e.g., Tousaint, 1978; Bourgois et al., 1982; Kerr et al., 1997; Vallejo et al., 2006; Kennan and Pindell, 2009) and active arc-continent collision (e.g., Keigwin, 1978; Kellogg and Bonini, 1982; Audemard, 1993; Taboada et al., 2000; Audemard, 2014). CASA project GPS campaign measurements from the late 1980s and early 1990s demonstrated the northeastward "escape" of the North Andes, Caribbean—North Andes convergence, and the ongoing rapid collision of the Panama arc with the North Andes (e.g., Kellogg et al., 1990; Freymueller et al., 1993; Trenkamp et al., 2002). Using GPS results from the first three CASA GPS campaigns (1988-1991), Freymueller et al. (1993) showed evidence for northward movement of the North Andes and convergence at the South Caribbean deformed belt. Kellogg and Vega (1995) used CASA GPS results to propose a rigid Panama block and rapid Panama-North Andes convergence. Trenkamp et al. (2002) presented CASA campaign data from 1991 to 1998 that showed wide plate boundary deformation and escape tectonics from the subducting Carnegie Ridge along an approximately 1400 km length of the North Andes, locking of the subducting Nazca plate and strain accumulation in the Ecuador-Colombia forearc, collision of the Panama arc with Colombia, and Caribbean-North Andes convergence.

Significant deformation in the region is driven by the aseismic Cocos Ridge subduction, Panama collision, and subduction of the Caribbean plate (e.g., van Benthem and Govers, 2010; DeMets et al., 2010; Kobayashi et al., 2014). Kobayashi et al. (2014), using GPS data from Panama, Costa Rica, and Colombia demonstrated that Panama acts as a single tectonic block, "escaping" eastward from the subducting Cocos Ridge, and colliding with the North Andes. Mora-Páez et al. (2016) measured velocities from nine continuous GPS (cGPS) sites and twenty campaign sites in the northeast trending Eastern Cordillera of Colombia, showing oblique convergence, consisting of 8 mm/yr of right-lateral strike-slip and only 4 mm/yr of northwest-southeast shortening.

In this chapter, we use a new compilation of volcanic age dates to revise the plate tectonic model for the northern Andes (50 Ma—Present). The age data provide important constraints on the locations of the Farallon/Nazca-Caribbean-South American triple junction, the locations and magnitude of normal Nazca and flat-slab Caribbean subduction, the geometry of the Panama-North Andes collision, and the origin of the Bucaramanga slab. We also relate "Laramide-style" basement orogenies to Caribbean flat-slab subduction and arc-continent collision and accretion. We also show how recent velocity vectors from continuously operating GPS reference sites (Mora-Páez et al., 2019) quantify margin-parallel "escape" driven by aseismic ridge subduction, slow Eastern Cordillera mountain building, and Choco arc accretion to the NAB.

2 Present tectonics of the North Andes (GPS vectors and profiles)

In this section, we review previous work including structural profiles by the first author (Fig. 1) and recently published GPS data (Fig. 2) from two of this chapter's authors (Kellogg and Mora-Páez) in Mora-Páez et al. (2019) to describe the Present tectonics of the North Andes. The three regional profiles were constrained by surface geology, gravity, and magnetic data, and well data, seismic reflection, and refraction profiles where available. The greatest sources or error in the interpretations were the limited seismic resolution and well control. Mora-Páez et al. (2019) estimated a new geodetic velocity field in the region of the North Andes using GPS data collected from 53 permanent stations in Colombia, Panama, and Ecuador (Fig. 2). This section covers Nazca and Caribbean subduction, arc-continent accretion, margin-parallel "escape," and mountain building.

2.1 Nazca subduction and volcanic arc

On the Pacific coast of Ecuador and Colombia, observed deformation includes a large contribution from elastic deformation due to the locked part of the Nazca oceanic subduction interface (Trenkamp et al., 2002; Kobayashi et al., 2014; Chlieh et al., 2014). Vallée et al. (2013) documented a long slow-slip event on a shallow locked patch along the Ecuador subduction interface using continuous GPS and broad-band seismic data. Slow-slip events may contribute to reduce the long-term moment deficit and postpone the failure of an asperity. Nocquet et al. (2014) used GPS data, primarily from Ecuador and Peru, to quantify the margin-parallel northeastward motion of the North Andean sliver or North Andean block (NAB) and the southeastward motion of the Peru sliver. Nocquet et al. (2017)

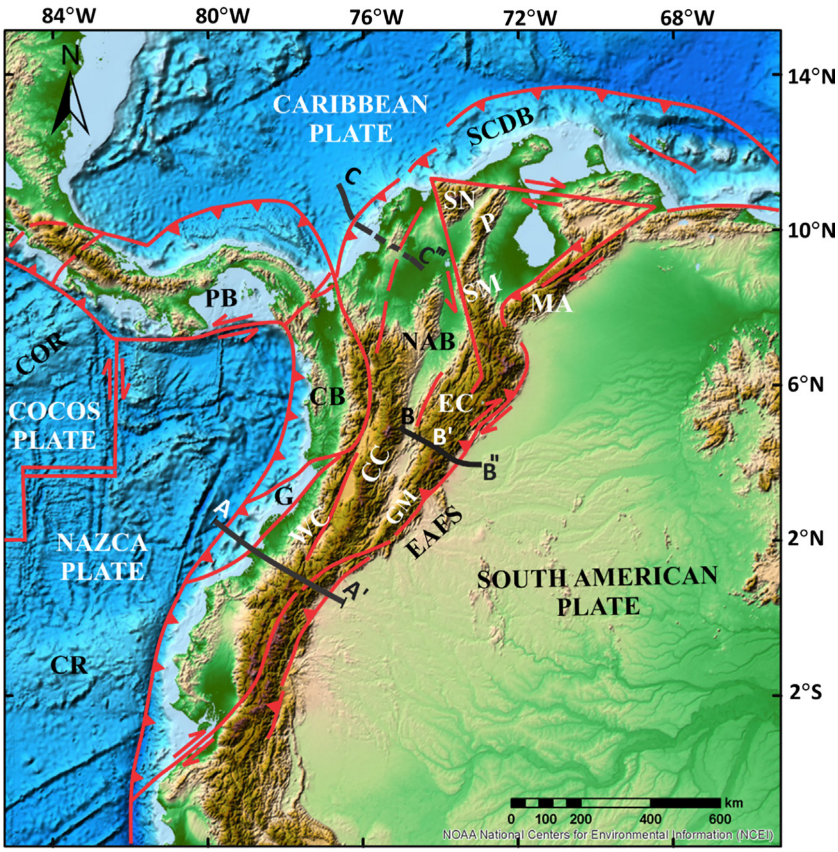

FIG. 1

Tectonic map of the north Andes, showing block and plate boundaries after Cediel et al. (2003), Tibaldi et al. (2007), Taboada et al. (2000), and Symithe et al. (2015). Abbreviations: *CB*, Choco block; *CC*, Central Cordillera; *COR*, Cocos Ridge; *CR*, Carnegie Ridge; *EAFS*, East Andean fault system; *EC*, Eastern Cordillera; *G*, Gorgona Island; *MA*, Merida (Venezuelan) Andes; *NAB*, North Andean block; *P*: Sierra de Perija; *PB*, Panama block; *SCDB*, South Caribbean deformed belt; *SM*, Santander Massif; *SN*, Sierra Nevada de Santa Marta; *WC*, Western Cordillera.

found that the coseismic slip in the 2016 Pedernales (Mw 7.8) earthquake exceeded the slip deficit accumulated since the last earthquake rupturing the same patch in 1942. Ye et al. (2016) modeled seismic and tsunami data and concluded that the moment for the great 1906 event was greater than the sum of the moments for the 1942, 1958, and 1979 events by a factor of three, and the 1906 earthquake ruptured asperities located trenchward of the subsequent events.

Sites on the Pacific coast of Colombia and Ecuador show substantial inland-directed motion relative to South America and the North Andes (Fig. 2; Mora-Páez et al., 2019). Near the Colombia-Ecuador border, coastal sites Esmeraldas (ESMR) and Tumaco (TUCO) moved eastward relative to the North Andes at 14.3 ± 0.3 mm/yr and 11.3 ± 0.6 mm/yr, respectively, prior to the April 16, 2016 M 7.8 Ecuador

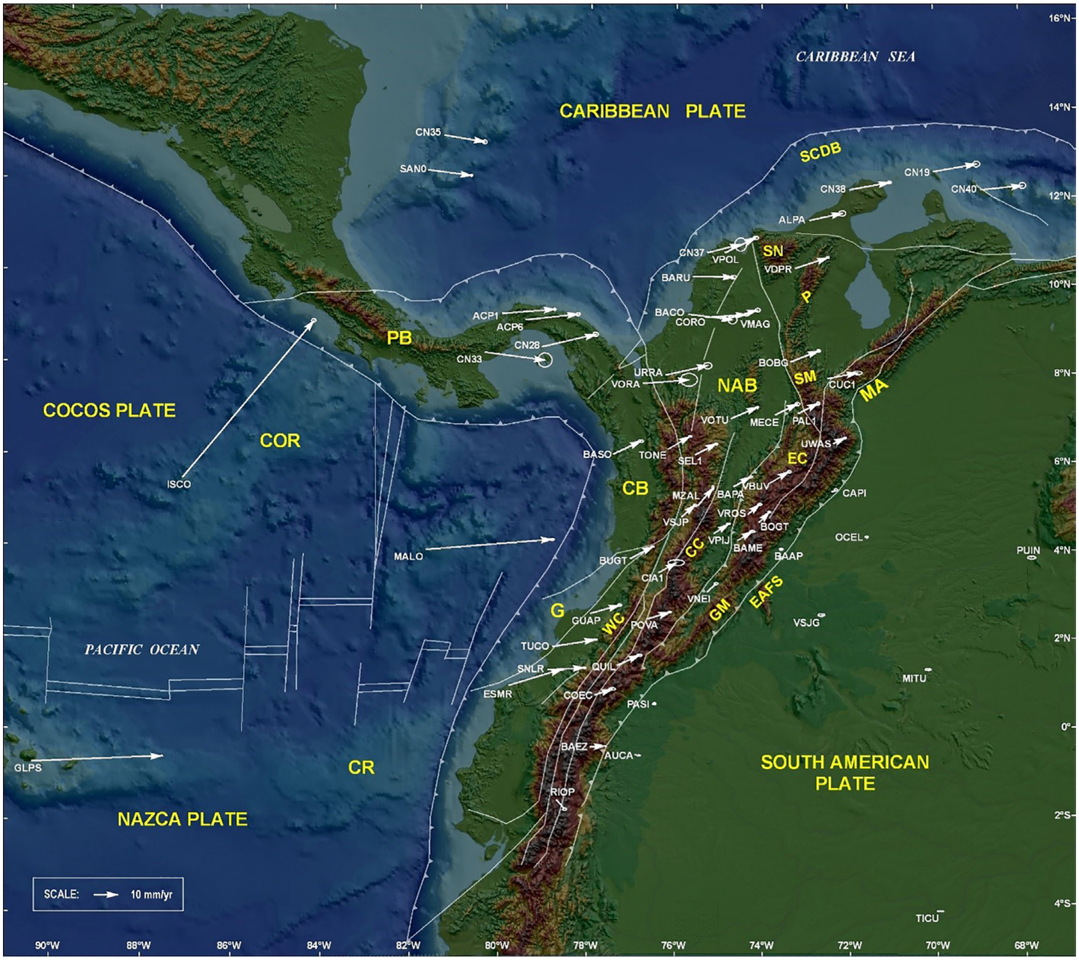

FIG. 2

GPS vectors relative to stable South America after Mora-Páez et al. (2019). 1 sigma error ellipses. *NAB*, North Andean Block; *EC*, Eastern Cordillera; *EAFS*, East Andean fault system; *SCDB*, South Caribbean deformed belt; *PB*, Panama Block; *BOGT*, Bogota; *SEL1*, Medellin; *QUIL*, Pasto; *TUCO*, Tumaco.

subduction earthquake. Kobayashi et al. (2014) obtained 100% coupling at the trench, decreasing to 50% by 20-km depth in a 3D model of elastic strain accumulation.

Just to the north at Guapi (GUAP), eastward movement at the coast drops to 4.2 ± 0.6 mm/yr. White et al. (2003) interpreted the reduction in apparent locking in southwest Colombia relative to northern Ecuador as the result of viscoelastic relaxation in the lower crust following the 1979 M_w 8.2 subduction earthquake. Inland and north of Guapi, our velocities have a substantially higher eastward component than the 1990s campaign velocities of Trenkamp et al. (2002), reflecting a possible decaying viscoelastic component or increased locking.

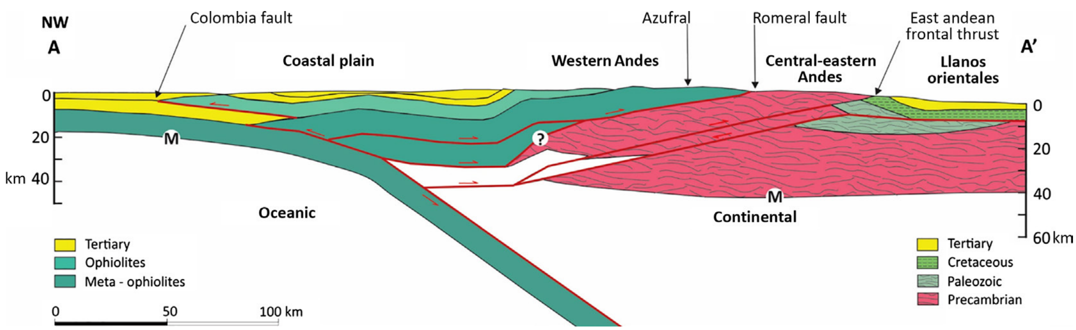

FIG. 3

Geological cross section A-A′ of the Andean margin of southern Colombia after Kellogg and Vega (1995) based on surface geology, and seismic refraction, gravity, and magnetic data from the Nariño Project (Meissner et al., 1976). Azufral, Azufral volcano; M, Moho boundary. No vertical exaggeration. For location see Fig. 1.

Based on surface geology and seismic refraction, gravity, and magnetic data from the Nariño Project (Meissner et al., 1976), Kellogg and Vega (1995) modeled the Nazca–North Andes plate boundary zone across the southern Colombian Andes (Fig. 3, profile A-A′). This profile illustrates the "normal" dip of the subducting Nazca oceanic slab, the position of Azufral volcano, and the structural geometry of obducted Caribbean oceanic terrane over continental crust of the South American margin. The 75-Ma Caribbean obduction is discussed further in this chapter (Section 4.1). Nazca subduction produces an active volcanic arc in Ecuador and Colombia. However, north of 5.5°N, arc volcanism is absent as the retreating low-angle to flat-subducting Caribbean slab forms a thermal blanket over the asthenospheric wedge (Malavé and Suárez, 1995; Taboada et al., 2000; Cortés and Angelier, 2005; Vargas et al., 2007; Prieto et al., 2012; Yarce et al., 2014; see Section 5.3).

2.2 Amagmatic Caribbean subduction and accretionary prism formation

San Andres and Providencia islands (SAN0 and CN35, two of the very few sites unequivocally located on the stable Caribbean plate) obliquely converge east-southeastward with stable South America at 18.4 ± 0.4 mm/yr and 17.3 ± 0.7 mm/yr, respectively (Fig. 2), and southeastward with respect to NAB at 13.2 ± 0.4 mm/yr and 12.5 ± 0.8 mm/yr, respectively (Mora-Páez et al., 2019). Slow amagmatic Caribbean subduction under the North Andes has been proposed by numerous authors based on a weak low-angle Wadati Benioff zone (e.g., Dewey, 1972; Kellogg and Bonini, 1982; Bernal-Olaya et al., 2015), seismic tomographic evidence for a low-angle southeastward-dipping, high-velocity slab (van der Hilst and Mann, 1994; van Benthem et al., 2013), seismic reflection profiles that show Caribbean acoustic basement underthrusting the deformed belt (e.g., Silver et al., 1975; Ladd et al., 1984; Bezada et al., 2010; Bernal-Olaya et al., 2015), and plate motion models that require convergence (Boschman et al., 2014; Kobayashi et al., 2014). The Boschman et al. (2014) plate reconstruction model requires continuous Caribbean subduction under the North Andes since the collision of the Caribbean Large Igneous Province and Great Arc of the Caribbean with northern South America 75 million years ago (Section 4.1.).

The Caribbean-North Andean margin was modeled with a 380-km-long composite transect of the Sinu-San Jacinto accretionary prism constrained by multichannel seismic profiles, potential fields, and surface and subsurface data from the North Colombia fold belt constrain (Fig. 4, profile C–C″';

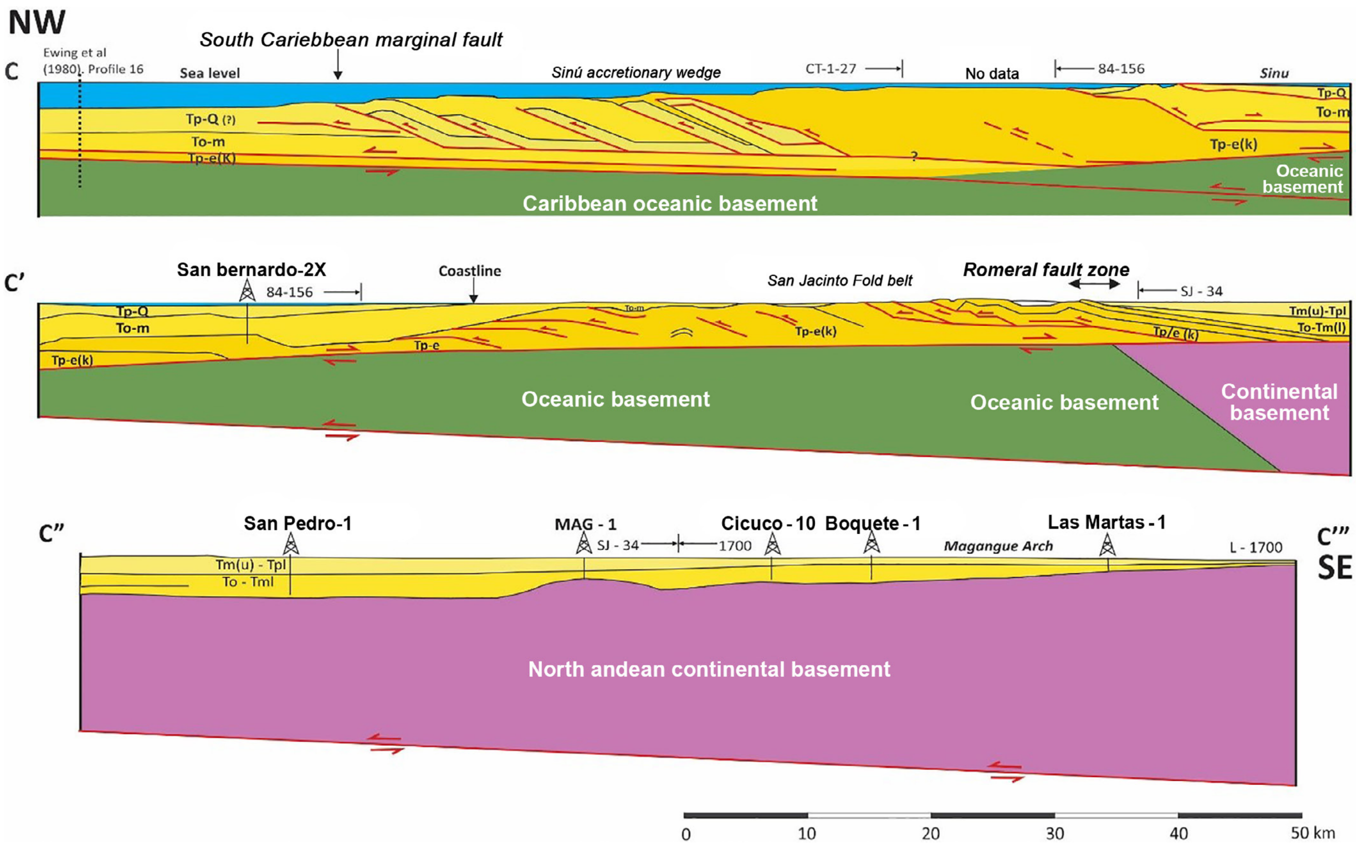

FIG. 4

Geological cross section C-C‴ of Sinu-San Jacinto fold belt and Magangue arch at the Caribbean-North Andean margin after Toto (1991) and Kellogg et al. (2005b). For location see Fig. 1.

Kellogg et al., 2005b). The Sinu-San Jacinto prism is a two-sided wedge that developed in response to Cenozoic compressional stresses at the Caribbean-North Andean convergent margin (Toto, 1991). Gravity and magnetic modeling predict northwest-dipping (8°–11°) crystalline basement beneath the wedge providing a rigid backstop or buttress. A blind east-verging backthrust near the sediment-basement interface is proposed to account for the slip on the west-verging thrusts near the Romeral fault zone. At depth, the Romeral fault is modeled as a steeply southeast-dipping (~45°) suture between oceanic and continental basement. The prism transect shows overall shortening of at least 110 km from 275 to 165 km accommodated by folding and thrusting. Folds have been formed over fault bends by thrusts that ramp up section from a decollement near the top of the Cretaceous with fundamental cutoff angles of 18–28°. The timing of the deformation is pre-Oligocene to middle Miocene in the San Jacinto belt and Quaternary to Pliocene in the Sinu belt. Application of a critically tapered wedge model to the observed prism geometry suggests that high pore pressures occur in the prism (Toto, 1991). Based on a tectono-stratigraphic study, Mora et al. (2018) concluded that the formation of the Lower Magdalena amagmatic, forearc basin occurred in a stable setting from the Oligocene to the present, characterized by the slow and nearly orthogonal, low-angle subduction of the Caribbean plateau.

The GPS velocity vectors suggest subduction-related deformation in the overriding North Andean block. Even though we estimate a significant eastward motion of the North Andean block relative to South America, Caribbean coastal sites still show large motions relative to the North Andes. CN38 and ALPA are moving eastward at 8.5 ± 0.8 mm/yr and 8.2 ± 0.9 mm/yr relative to the North Andes (Mora-Páez et al., 2019). The orientation of the vectors is very similar to the motion of sites in Panamá relative to the North Andes.

Despite the long-lived Caribbean subduction beneath the North Andes, no volcanic arc has formed. The lack of magmatic activity at other flat to low-angle subducting margins has been attributed to the lack of an asthenospheric wedge and resulting low heat flow (e.g., Pilger, 1981, and Jordan et al., 1983). Later in Section 5.1, low-angle subduction of the buoyant Caribbean plate is also linked to basement block uplifts in the northern Andes.

2.3 Arc-continent collision

The Panama-Choco arc is the southwest boundary of the buoyant Caribbean plate, which has been underthrusting the North Andes for the last 75 Myr. The initial collision of the Panama-Choco arc and the North Andes occurred between 12 and 40 Ma (e.g., Duque-Caro, 1990; Coates et al., 2004; Montes et al., 2012; Barat et al., 2014; León et al., 2018). Montes et al. (2015) used cooling ages of magmas, U/Pb dating, paleomagnetic pole rotations, and Atlantic sea-floor anomalies to propose that closure of the Isthmus of Panama occurred at 15 Ma. Coates and Stallard (2013) propose that the Indonesian Australian Archipelago provides a model for the Panama Arc between 15 and 3 Ma that accounts for the tectonic configuration, while also accounting for the marine fossil record, and the delayed Great American Biotic Interchange.

The Panamá arc is rapidly colliding eastward with the North Andean block (NAB) at approximately 16-17 mm/yr (Mora-Páez et al., 2019). The present deformation associated with the Panama arc collision is confined to the North Andes north of 7.5°N latitude. VORA (Fig. 2, Atrato), for example, is moving eastward with the collision at 13.0 ± 1.8 mm/yr relative to NAB. BASO (Choco), however, just 200 km to the south, is moving eastward at only 4.3 ± 1.0 mm/yr (Mora-Páez et al., 2019). In Section 5, we propose that the Panamá Choco arc collided with the North Andes, acting as a rigid indenter. Subsequently, the Choco arc broke off of the indenter and was accreted to the North Andean block.

The Colombia-Panamá border area is a zone of active seismicity. In 1992, two large shallow earthquakes occurred in the area ($M_S = 6.6$ and 7.3; Wallace and Beck, 1993), and the focal mechanisms are consistent with compression normal to the Panamá-North Andes suture (Freymueller et al., 1993). A recent earthquake occurred on September 14, 2016, in the Mutatá region (Mw = 6.0, depth = 18 km) with a focal mechanism consistent with northwest-southeast compression (USGS National Earthquake Information Center). Geodetic evidence for active Panama-North Andes collision was first reported by Kellogg and Vega (1995) and Mora-Páez (1995). Kobayashi et al. (2014) interpret the eastward motion of the Panama block as tectonic escape from the subducting Cocos Ridge at the Middle America trench and modeled the Panama Block-NAB convergence as 12.2 mm/yr to the southeast (124°).

Since the Panamá-North Andes convergence zone involves the collision of two thick buoyant crustal blocks, the resulting deformation is collision-like, unlike subduction zones where most of the convergence in the overriding plate is recoverable elastic strain associated with the earthquake cycle. Our new vectors are consistent with the Trenkamp et al. (2002) model for Panamá collision related deformation in northern Colombia over a locked east-dipping thrust fault zone. The Pérez et al. (2018) estimate of rapid eastward slip of the NAB relative to South America (15.0 ± 1.0 mm/yr) reflects deformation related to the Panamá collision.

2.4 Margin-parallel "escape"

McCaffrey (1996) has shown that about half of all modern subduction zones have mobile forearc blocks. Slip partitioning into margin-parallel and margin-normal components within the overriding plate at oblique subduction zones frequently results in lithospheric blocks being detached from the overriding plate. The forearc blocks are driven by plate coupling and are displaced relative to the overriding plate (McCaffrey, 2002).

By the early Pleistocene, in addition to the compressional stress regime, a NE-SW strike-slip component was introduced as the northern Andes began to "escape." Egbue and Kellogg (2010) compiled field geologic estimates of northeastward displacement rates for the North Andes with a mean estimated geologic slip rate for the last 86,000 years of 7.6 mm/yr. Egbue and Kellogg (2010) cite the earliest measurements dating back to the opening of the Gulf of Guayaquil at 1.8 Ma, although Benítez (1986) claims evidence for extension starting at the Miocene-Pliocene boundary. The northeastward displacement of the North Andes has been interpreted as tectonic escape from the Carnegie Ridge subducting at the Ecuador trench (Egbue and Kellogg, 2010; Nocquet et al., 2014; Chlieh et al., 2014). About 2 Ma, the aseismic Carnegie ridge, which was formed by the Galapagos hotspot, arrived at the Colombia-Ecuador trench (Lonsdale and Klitgord, 1978; Pedoja, 2003; Cantalamessa and Di Celma, 2004), and initiated the northeastward "escape" of the northern Andes (Egbue and Kellogg, 2010). Presently, in the Eastern Cordillera, the escape rate (8.1 mm/yr dextral slip on the EAFZ) is greater than the rate of range-normal shortening (4.3 mm/yr).

At least ten sites in the North Andes (BAPA, CIA1, MECE, MZAL, POVA, QUIL, SEL1, VPIJ, VROS, VSJP) have margin-parallel vectors insignificantly different at the 95% confidence level from 8.6 ± 1.0 mm/yr, the estimated average motion of the North Andean block (8.6 mm/yr toward 060°, Mora-Páez et al., 2019). This NAB vector can be resolved into a margin-parallel (035°) component of 8.1 mm/yr and a margin-normal component of 4.3 mm/yr. Mora-Páez et al. (2016) estimated right-lateral strike-slip shear along the northeast trending Eastern Cordillera of 8.0 ± 1.7 mm/yr. Most of the northeastward "escape" is accommodated along the broad East Andean Fault System (EAFS; e.g., Schubert and Henneberg, 1975; Ego et al., 1996; Audemard et al., 1999; Tibaldi et al., 2007; Egbue and Kellogg, 2010).

2.5 Margin-normal mountain building

The margin-normal (125°) components of the new GPS vectors relative to stable South America vary from 1.8 to 15.6 mm/yr (Mora-Páez et al., 2019). There are much greater variations in margin-normal displacement in the North Andes than variations in margin-parallel displacement, because margin-parallel vectors are dominated by escape-related translation while margin-normal vectors are dominated by the subduction earthquake cycle and permanent deformation (mountain building). Mountains are built by both viscous/plastic deformation and short-term elastic deformation. Compressive mountain belts, such as the Eastern Cordillera of Colombia, are primarily built by slip on reverse faults (e.g., Fig. 9, Kellogg et al., 2005a).

Profile B-B″ (Fig. 5) extends from the Central Cordillera, across the Middle Magdalena basin, the Villeta and Cocuy anticlinoria of the Eastern Cordillera and Foothills Belt, to the Llanos foredeep basin. The geological model was controlled by surface geology (Cardozo-Puentes, 1988; Namson et al., 1994 (Guaduas syncline); Ingeominas maps and unpublished reports), 6 wells (Armero-2, Ocobo-1, Villavicencio-1, 1127-X, Ocoa-1, Austral-1), over 130 km of seismic reflection profiles (AV-83-15, GB-78-1, C-79-18, BPT-87-5, V-88-1236), and gravity and magnetic models (Duque, 1994; Kellogg et al., 2005a). Conservation of rock volume and layer-parallel folding were assumed (e.g., Woodward et al., 1989), and Kellogg et al. (2005a) estimated total shortening on reverse faults as 110–150 km. The profile shows "thin-skinned" thrust faults ramping up from horizontal decollement horizons in the Lower Cretaceous, followed by "thick-skinned" basement faulting forming monoclines and thrusts on deep crustal ramps in the Pre-Cretaceous basement (e.g., Egbue and Kellogg, 2012), especially on the southeastern flank (Villavicencio).

Earthquake focal mechanisms for the Eastern Cordillera are characterized by WNW-ESE compression on reverse faults (e.g., Taboada et al., 2000; Corredor, 2003; Cortés and Angelier, 2005). Both seismic and aseismic slip on the reverse faults produces horizontal shortening and vertical thickening (permanent deformation). The rate of mountain growth depends on the rate of shortening, the erosion rate, the dip of the thrust faults, and isostatic adjustments of the crust to the mountain load. Using an elastic half-space model for the Ecuador trench, Trenkamp et al. (2002) estimated 6 mm/yr permanent shortening on reverse faults in the Ecuadorian Andes along an east-west profile. Of this, recoverable elastic trench-related displacement is 1–2 mm/yr (Trenkamp et al., 2002). Explanations for the apparent discrepancy between this small margin-normal shortening and evidence for recent rapid uplift of the Eastern Cordillera are presented in Section 5. Rapid margin-normal shortening of 9–14 mm/yr in northern Colombia north of 7° N reflects mountain building and seismic hazard across the broad plate boundary, including the Western and Central cordilleras of Colombia and the Merida Andes of Venezuela (e.g., Kellogg and Bonini, 1982; Audemard and Audemard, 2002). The permanent shortening in northern Colombia and Venezuela is driven by the Panamá collision and Caribbean flat slab subduction.

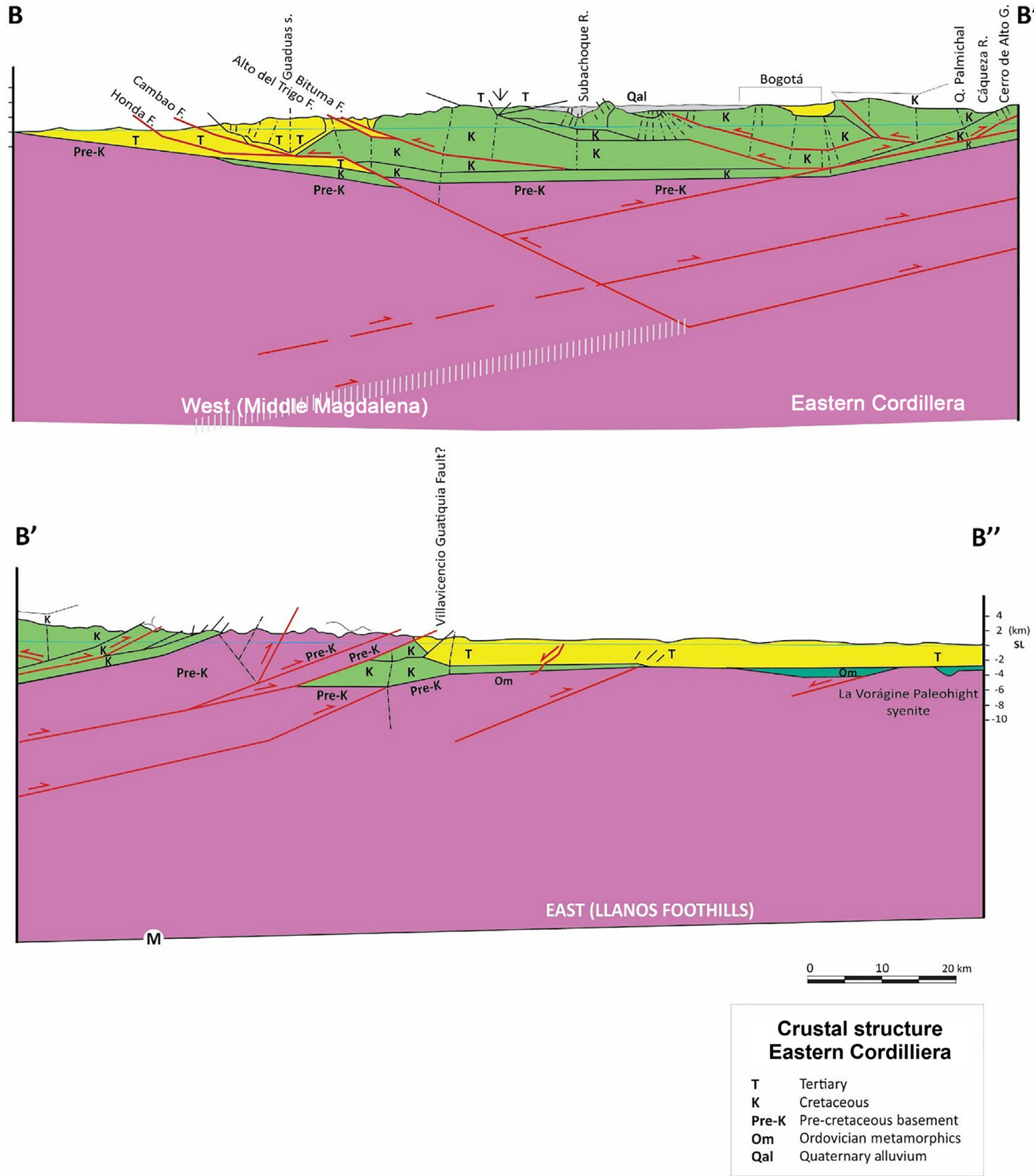

FIG. 5

Geologic cross section B-B″ of the Eastern Cordillera after Kellogg et al. (2005a). M, Moho boundary. No vertical exaggeration. For location see Fig. 1.

3 Data sources and methodology

3.1 Radiometric ages for arc volcanics

We compiled ages of igneous rocks following the strategy of Wagner et al. (2017) to use the volcanic arc ages to locate the temporal positions of normal versus flat slab subduction. The Wagner et al. (2017) compilation dates back to 14 Ma. In this study, one goal was to define plate geometries before and during the Panama arc-South America collision, which may have begun as early as 28 Ma (Montes et al., 2012), so we compiled a comprehensive dataset of 1100 radiometric ages extending back to 100 Ma. Supplementary Data, Table 1 in the online version at https://doi.org/10.1016/B978-0-12-816009-1.00006-X includes 249 ages for rocks from Colombia and Panama younger than 50 Ma, along with their errors, dating methods, type of rock, latitude and longitude, and references. The dated rocks correspond to pyroclastic flows, porphyritic bodies, plutonic bodies, and tuffs. Only U-Pb, K-Ar, and 40Ar-39Ar ages were included in this compilation. Fission track ages were not included, as they may represent episodes of heating instead of igneous crystallization. For plutonic bodies, only ages interpreted as crystallization ages by the original authors were used. The Colombian radiometric ages are from Servicio Geológico Colombiano (Gómez-Tapias et al., 2013). The Panama ages were obtained from Roy (1988), Lissinna (2005), and Wegner et al. (2011). We then mapped the volcanic arc rock ages and locations (Fig. 6) to constrain the northward migration of the normal dipping Farallon/Nazca subducting slab and Farallon-Caribbean-South America triple junction in our plate tectonic reconstructions.

3.2 Revised plate tectonic model

Fig. 7 shows the plate tectonic kinematic model of Boschman et al. (2014) modified in the area of the North Andes based on our compilation of volcanic ages for Colombia and Panama, the segmentation and rotation of the Panama-Choco island arc (Montes et al., 2012), shortening in the Eastern Cordillera (Kellogg et al., 2005a), and northeastern "escape" of the North Andean Block (Egbue and Kellogg, 2010). Red dots show sample locations for volcanic arc rocks with radiometric age dates in each time period from Fig. 6. The revised model (Fig. 7) focused on the relative locations of the Caribbean, South American, Nazca, and Farallon plates during the last 50 million years. During its tectonic evolution, the Caribbean plate was largely surrounded by subduction and transform boundaries, making quantitative relative plate motion models difficult. Our reconstruction of the kinematic evolution of the Caribbean plate began with the model of Boschman et al. (2014). Pindell and Barrett (1990) and Ross and Scotese (1988) provided poles for a large number of tectonic elements in the Caribbean region, using seafloor spreading poles in the Central and South Atlantic (Klitgord and Schouten, 1986). Magnetic spreading anomalies for the Cayman Trough (Rosencrantz and Sclater, 1986; Rosencrantz et al., 1988) are particularly important for quantifying relative Caribbean-North American displacement over the last 50 Myr. The Boschman et al. (2014) model used the magnetic anomaly picks of Leroy et al. (2000). Qualitative tectonic reconstructions for the Caribbean include Burke (1988), Pindell et al. (1988), Meschede and Frisch (1998), Müller et al. (1999), and Pindell and Kennan (2009). Parameters to constrain our revision of the Boschman et al. (2014) plate model, including the timing of the Panama arc collision, shortening in the Eastern Cordillera, and northeastern "escape" of the North Andean Block (NAB) are listed in Supplementary Data, Table 2 in the online version at https://doi.org/10.1016/B978-0-12-816009-1.00006-X. We used the freely available software package GPlates (http://www.gplates.org; Boyden et al., 2011) to convert geological data and interpretations into Euler poles and finite rotations.

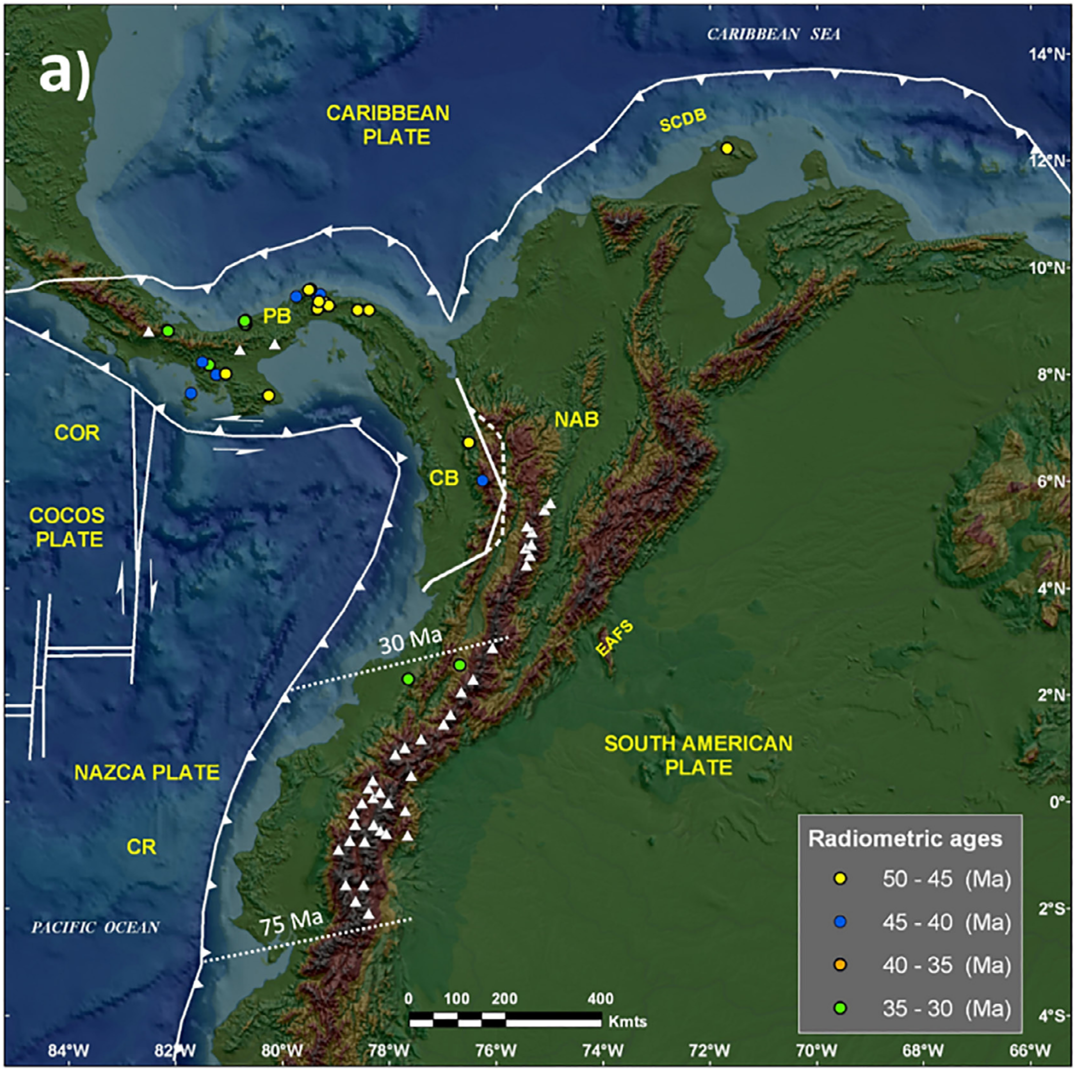

FIG. 6

Locations of radiometric age locations for arc volcanics for Colombia and Panama after Franco (2017). (A) 30–50 Ma. (B) 0–30 Ma. Sample parameters are in Supplementary Data, Table 1 in the online version at https://doi.org/10.1016/B978-0-12-816009-1.00006-X. Active volcanoes *(white triangles)*. Choco terrane boundary from gravity and magnetics *(solid white line)*, Cediel et al., 2003 *(dashed line)*. Locations of northern edge of Farallon/Nazca slab at 75, 30, and 20 Ma based on radiometric ages of arc volcanics and age of accretion of western Cordillera in Ecuador.

(Continued)

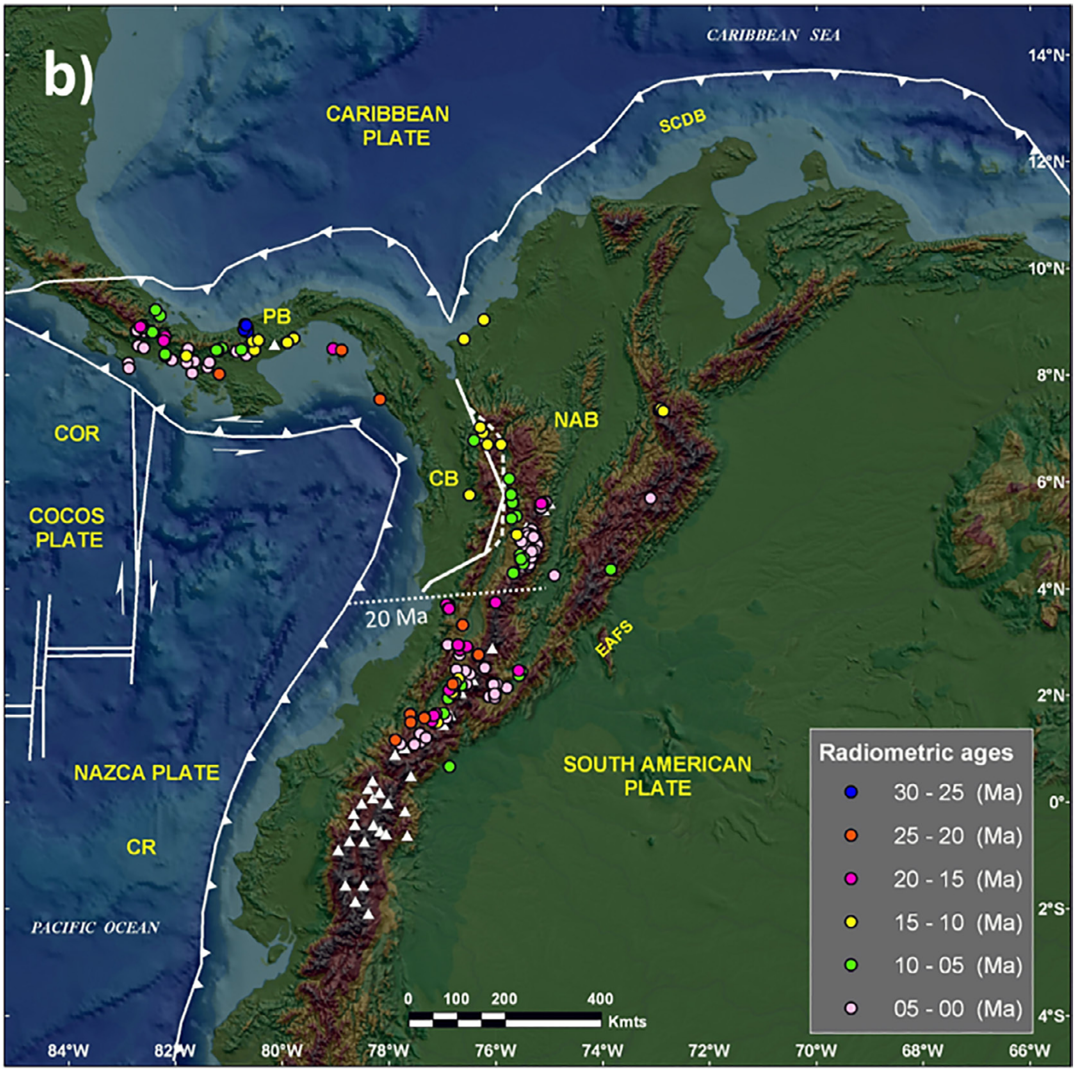

FIG. 6—CONT'D

In this chapter, we use a compilation of volcanic arc age data (Fig. 2, Supplementary Data, Table 1 in the online version at https://doi.org/10.1016/B978-0-12-816009-1.00006-X) to constrain the location of the northward migrating Farallon-Caribbean-South America triple junction. The location of this triple junction is very important to predict the location of the low-angle or flat subducted Caribbean plate beneath northern South America. Also, the kinematic plate motion model presented here includes a realistic estimate of the segmentation and rotation of the Panama-Choco island arc from 38 Ma to Present following the reconstruction of Montes et al. (2012) based on paleomagnetic rotations.

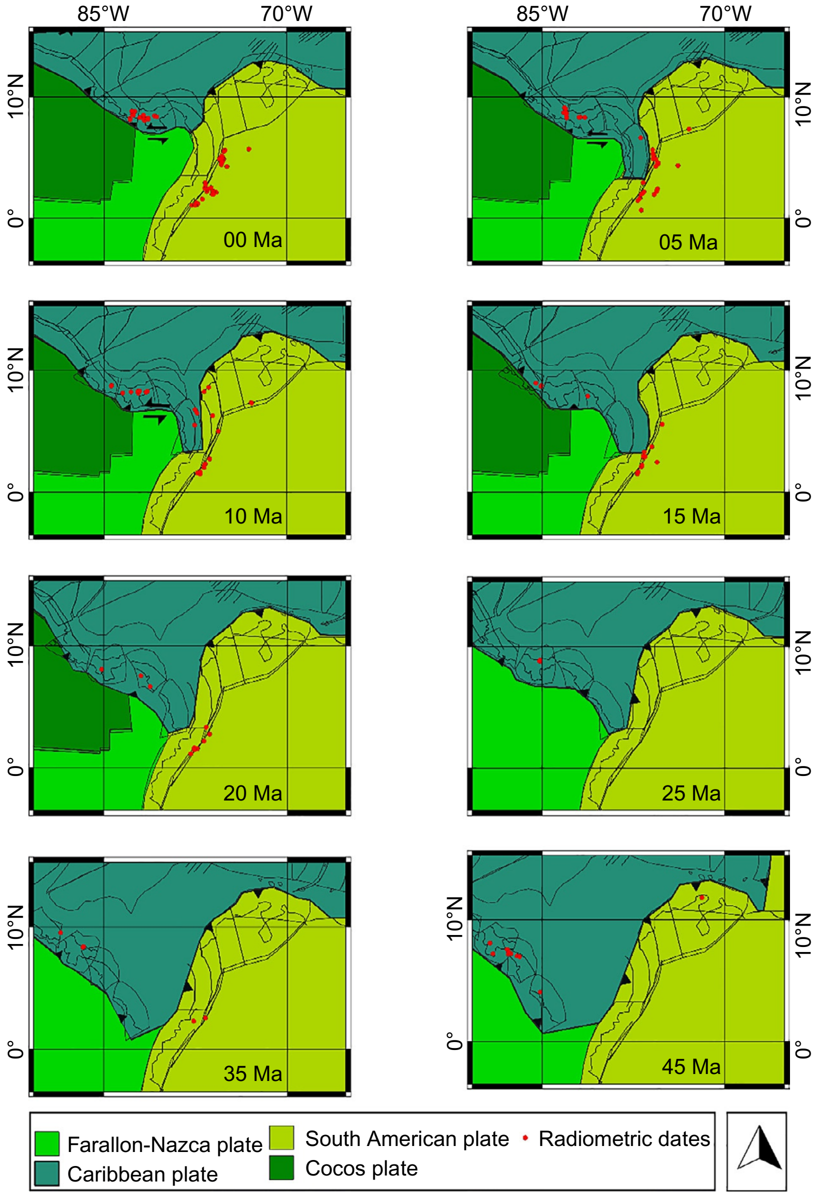

FIG. 7

Caribbean North Andean plate reconstruction 45 Ma to Present showing block and plate boundaries revised after Boschman et al. (2014) and Franco (2017). *Red dots* show locations of radiometric age locations for arc volcanics (Fig. 2, Supplementary Data). Locations of Farallon/Nazca-Caribbean-North Andes triple junction are revised based on northernmost radiometric ages of arc volcanics (Fig. 6). Panama Choco block rotations after Montes et al. (2012).

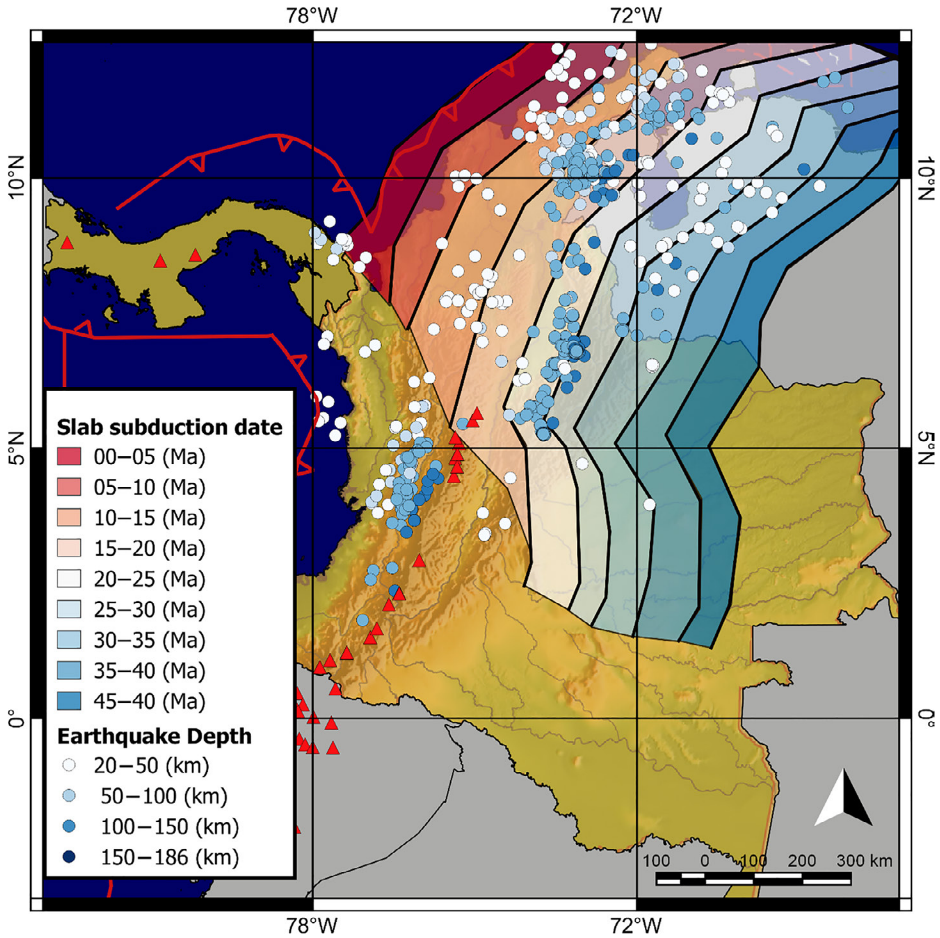

FIG. 8

Map of Caribbean slab age (since subduction) and seismicity after Franco (2017). Hypocenter locations compiled from the International Seismological Center (ISC), Fundación Venezolana de Investigaciones Sismológicas (FUNVISIS), and La Red Sismológica Nacional de Colombia (RSNC). Note that the deepest Caribbean slab earthquakes occur at slab ages of 25 Ma or less. Also note that the southern limit of flat slab seismicity at 5.5°N coincides with the southern limit of Caribbean slab subducted in the last 20 Myr. Lack of seismicity in lithosphere subducted >25 Myr ago may be due to thermal equilibration or delamination.

3.3 Earthquake hypocentral locations

Earthquake hypocentral locations are used to locate the positions of present-day subducting slabs. Fig. 8 shows seismicity compiled from the International Seismological Center (ISC, 2013; mb > 4.5; 1980–2013), Fundación Venezolana de Investigaciones Sismológicas (FUNVISIS, 2017; mb >3; 2003-2012), and the National Network of the Colombian Geological Survey (Red Sismológica Nacional de Colombia, RSNC, 2017; mb >4; 2011–2017). FUNVISIS data were used for western Venezuela, and

RSNC data was used for Colombia. The large number of hypocenters in the FUNVISIS catalog for events shallower than 50 km obscured the intermediate depth seismicity, so some shallow earthquakes were omitted.

4 Plate tectonic evolution of the North Andes

4.1 75 Ma–45 Ma, Previous work—Caribbean obduction—Western Cordillera

The Caribbean Large Igneous Province (CLIP) first collided with South America at ~75 Ma, resulting in the detachment and clockwise rotation of allochthons that form the present-day basement of the forearc plains and the Western Cordillera (Spikings et al., 2015). Convergent motion resulted in the obduction of CLIP magmas eastward over continental crust of the South American margin in Ecuador and Colombia (Tousaint, 1978; Bourgois et al., 1982; Kerr et al., 1997; Vallejo et al., 2006; Kennan and Pindell, 2009). Based on surface geology and seismic refraction, gravity, and magnetic data from the Nariño Project (Meissner et al., 1976), Kellogg and Vega (1995) modeled the transpressive suture as a low-angle ~10–15° west-dipping "paleo-Romeral" thrust fault with at least 70 km of shortening (Fig. 3, profile A-A′). The accreted Western Cordillera oceanic terrane was derived from the Caribbean plate and continuous with the Aves Ridge terrane (Fig. 12 in Pindell and Barrett, 1990). The Western Cordillera terrane was an island arc south in Ecuador and an immature oceanic island arc (e.g., Barrero, 1977; McCourt et al., 1984) or oceanic crust (Bourgois et al., 1982) north in Colombia. Following the accretion of the Western Cordillera terrane, subduction polarity flipped to east-dipping under the North Andes, the trench jumped west of the accreted terrane, and Caribbean lithosphere began subducting under the northern Andes.

In the Boschman et al. (2014) plate reconstruction, 50% of the Caribbean plate at 70 Ma (~$1.8 \times 10^6 km^2$) has been subsequently subducted under northwestern South America during the Cenozoic. The Caribbean-Farallon-South America triple junction was located south of the NAB at approximately 7°S at the beginning of the Paleocene (70 Ma) to account for the accretion of the Western Cordillera oceanic terrane (Boschman et al., 2014), and the Caribbean plate extended at least 1500 km along the entire western boundary of the North Andean Block (NAB).

4.2 45 Ma to 25 Ma—Revised model—Farallon-Caribbean-North Andes triple junction

Fig. 7 shows the Boschman et al. (2014) kinematic plate reconstructions beginning at 45 Ma modified to show the locations of the Farallon/Nazca-Caribbean-North Andes triple junction based on northernmost radiometric ages of arc volcanics (Fig. 6). Fifty million years ago, the Caribbean plate ran into the Bahamas Bank on the North American plate and its motion relative to the American plates changed dramatically (Boschman et al., 2014). In the past 50 million years, the Caribbean has moved 1000 km eastward relative to the North and South American plates. In the hot spot absolute motion reference frame, the Caribbean has been fairly stationary, while the North and South American plates have been moving westward (van der Meer et al., 2010). Note that approximately one-third of the Caribbean plate has been subducted under northwestern South America in the last 45 million years. Also about 45 Ma a second Late Cretaceous oceanic plateau, the Gorgona Plateau (Fig. 1), containing the only known Phanerozoic komatiites, collided with and was accreted to the north Andean margin (Kerr and Tarney, 2005).

In our compilation of volcanic or plutonic radiometric age dates in western Colombia, there were only 3 age dates from 55 Ma to 25 Ma (Supplementary Data, Table 1 in the online version at https://doi.org/10.1016/B978-0-12-816009-1.00006-X), and no ages from 50 to 35 Ma (Fig. 6A). There are two ages from 40 to 50 Ma in the Choco arc (Fig. 6A) related to Farallon plate subduction. The Choco arc had not yet collided with the North Andean margin. The lack of a volcanic arc in the north Andes from 55 to 25 Ma suggests that the Caribbean plate was buoyant and subducting amagmatically at a low angle under South America as it is at present. At 45 Ma, the southern tip of the Choco volcanic island arc was located 400–500 km west of South America on the southwest trailing margin of the Caribbean plate. Based on nine radiometric ages for volcanic rocks, the Panama arc (one age in Choco) was very active between 45 and 50 million years ago. We speculate that the increased volcanic activity may have been related to the Caribbean-Bahamas collision at 50 Ma and a resultant increase in the relative Farallon-Caribbean convergence rate south of Panama.

By 32 Ma, following an apparent volcanic age gap of 15–20 Myr, two radiometric ages were recorded for volcanic and plutonic rocks in southern Colombia (Fig. 6A, present latitude ~2.3°N). This renewed volcanic activity may have marked the northward advance of the Farallon-Caribbean-South America triple junction as Farallon plate "normal" magmatic subduction began under the northern Andean margin (Fig. 7).

4.3 25 Ma to Present—Revised model—Panama-Choco arc-continent collision

Fig. 7 shows revised Boschman et al. (2014) kinematic plate reconstructions. Revisions include segmentation and rotation of the Panama-Choco island arc from 38 Ma to Present after Montes et al. (2012).

Volcanic arc activity resumed in southern Colombia by 20 Ma, extending as far north as 3.6° N (Fig. 6B). This new arc volcanism suggests that the Farallon-Caribbean-South America triple junction continued to move northeastward up the north Andean margin at an approximate rate of 12 km/Ma (Figs. 6 and 7). At 23 Ma, the Cocos plate split off from the reduced Farallon plate (Fig. 7), which was renamed the Nazca plate initiating Cocos-Nazca spreading (Lonsdale, 2005). Relative plate convergence at the southern Colombia trench changed from northeastward Farallon motion to more eastward Nazca convergence (Lonsdale and Klitgord, 1978).

The Panama-Choco arc is the southwest boundary of the buoyant Caribbean plate, which has been underthrusting the North Andes for the last 75 Myr. The initial collision of the Panama-Choco arc and the North Andes occurred between 12 and 40 Ma (e.g., Duque-Caro, 1990; Coates et al., 2004; Montes et al., 2012; Barat et al., 2014; Montes et al., 2015; León et al., 2018).

Volcanic activity continued in western Panama from 35 Ma to Present. Few ages are available in this time period for eastern Panama and Choco until 15 million years ago. A spike in age dates (17 age dates) in the Choco terrane and just east of the terrane from 15 to 5 Ma (Fig. 6B) seems to bracket the initial Panama-Choco-North Andes collision. The collision may have detached Choco from the Caribbean plate, increasing relative Nazca-Choco convergence rates and arc activity. Shallow Caribbean subduction continued east of the Choco arc under the North Andes until the final arc-continent accretion. Five million years ago, volcanic activity abruptly ended again north of 5.5°N. We propose that this occurred as the subducting Nazca lithosphere underthrust the shallow-dipping retreating Caribbean slab. The retreating Caribbean slab then formed a thermal blanket over the Panama-Choco asthenospheric wedge (e.g., Taboada et al., 2000).

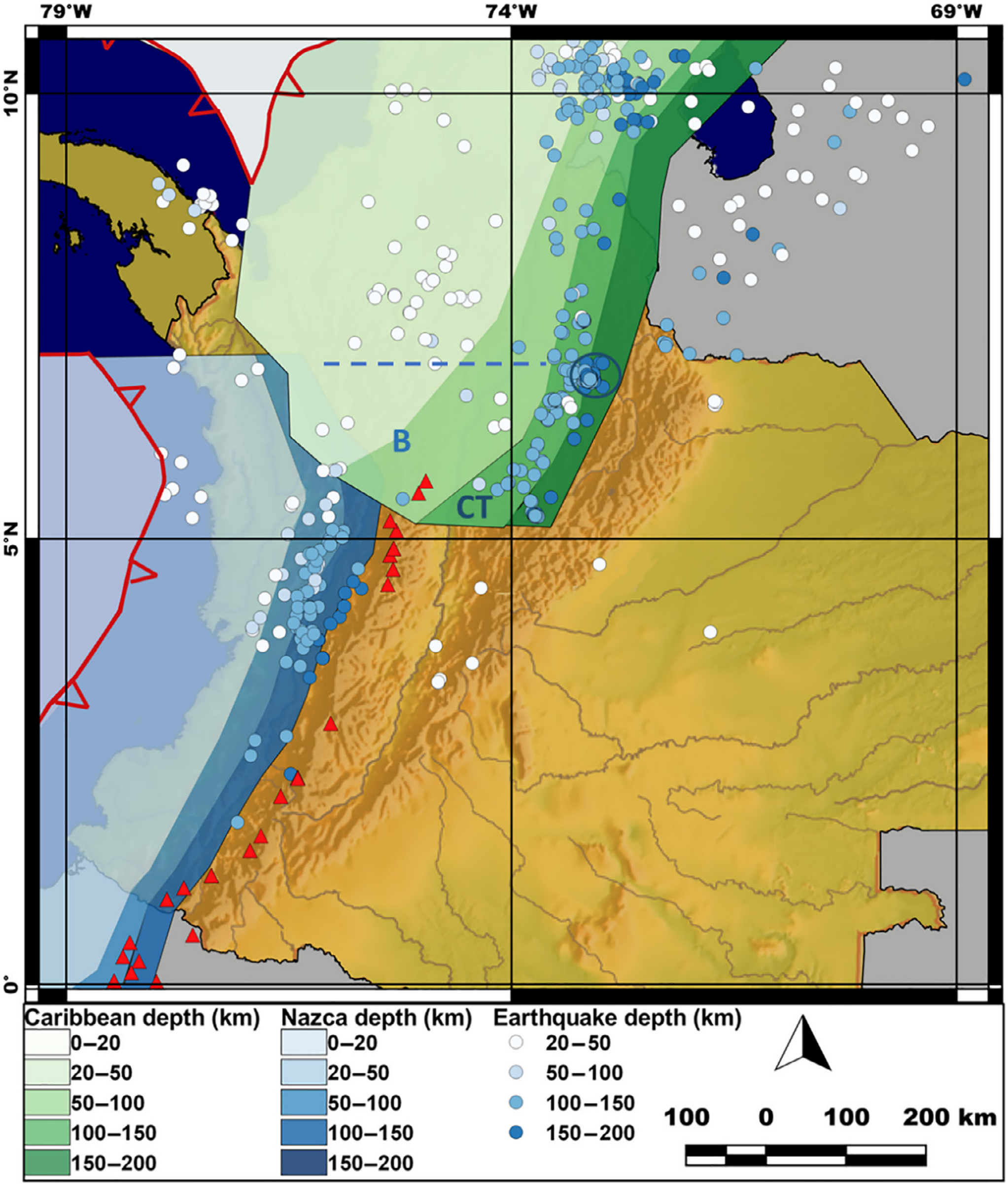

FIG. 9

Slab depths and predicted locations of Caribbean and Nazca slab boundaries based on seismicity and location of quaternary arc volcanoes after Franco (2017). *B*, Bucaramanga segment; *CT*, Caldas "Tear"; *circle*, Bucaramanga nest. South of the CT we predict that the older Caribbean slab has delaminated or thermally equilibrated.

Fig. 8 shows the predicted present-day position of the subducted Caribbean slab based on our plate reconstruction (after Franco, 2017). Also shown is the relative subduction age of the Caribbean slab and the associated seismicity. Note that the deepest Caribbean slab earthquakes occur in slabs subducted about 25 Ma. Also note that the lack of flat slab seismicity south of 5°N latitude coincides approximately with the predicted lack of Caribbean slab subducted in the last 20 Myr. The lack of seismicity in sections of the Caribbean slab subducted >25 million years ago may be the result of thermal equilibration or delamination.

Fig. 9 shows the predicted location of present-day Caribbean and Nazca slab boundaries based on seismicity, our plate reconstruction, and the location of Quaternary arc volcanoes (Franco, 2017). In our model, the Nazca slab is underthrusting the relict Caribbean slab for 200 km northward from 5°N to 7°N. We will explore this topic further in Section 5.

5 Discussion

5.1 Flat slab subduction, low heat flow, and thick-skinned basement tectonics

Flat slab subduction is often characterized by a lack of a volcanic arc because there is no asthenospheric wedge in the overriding plate, with resultant low heat flow, and rigid thick-skinned "Laramide" style basement tectonics (e.g., Smithson et al., 1978; Saleeby, 2003; DeCelles, 2004; Liu et al., 2008; Miller and Mitra, 2011; Fan and Carrapa, 2014). The basement block, "germanotype," or "thick-skinned" tectonic style of the Laramide orogeny in the central and southern Rocky Mountains of the United States was characterized by broad zones of uniform strike and dip separated by narrow zones of steeper dips or high-angle faults. The uplifts have Bouguer gravity anomaly highs, indicating that dense basement rocks are involved and that the uplifts are "rootless," i.e., without crustal thickening. Examples of "thick-skinned" basement tectonics are found throughout the Laramide US Rocky Mountains (e.g., Smithson et al., 1978; Miller and Mitra, 2011) and the Sierras Pampeanas in Argentina (Jordan and Allmendinger, 1986; Ramos et al., 2002; Fan and Carrapa, 2014), as well as in the northern Andes (e.g., Kellogg and Bonini, 1982; De Toni and Kellogg, 1993).

Prior to the basement Laramide orogeny in the US Rocky Mountains, the region was the site of a Cordilleran foreland basin associated with thin-skinned deformation and flexural loading of a fold-and-thrust belt. Subsequent thick-skinned deformation (Laramide orogeny) partitioned the regional foreland basin and caused >4 km of localized exhumation of crystalline basement blocks, accompanied by localized subsidence of intermontane basins. It is generally accepted that the switch of deformation style from thin skinned to thick skinned was caused by the change from normal high-angle subduction to low-angle subduction of buoyant Farallon oceanic lithosphere beneath western North America (e.g., Saleeby, 2003; DeCelles, 2004; Liu et al., 2008; Fan and Carrapa, 2014).

The Cenozoic orogenic evolution of the northern Andes included numerous Laramide-style basement uplifts, correlating with Caribbean flat slab subduction. Cooling and exhumation rates in the Central Cordillera suddenly increased in the Middle Eocene 45–40 Ma (~0.8 km/Ma) signaling basement uplift (Villagómez and Spikings, 2013). To the east, an early to middle Eocene (56–42 Ma) basement uplift also occurred in the Garzon Massif (Fig. 1) (Saeid et al., 2017). During this time, there was no active volcanic arc and the Caribbean plate was subducting along the entire western north Andean margin (Fig. 3), except for the collision and accretion of a Gorgona plateau fragment ~ 45 Ma (Kerr and Tarney, 2005).

In the Late Oligocene (~ 25 Ma), basement deformation began in the Sierra de Perija (Kellogg, 1984), Santander Massif (Amaya et al., 2017), the northern Eastern Cordillera (Corredor, 2003), and the Sierra Nevada de Santa Marta (Villagómez et al., 2011) (Fig. 1). The Caribbean plate was subducting under the entire western margin of the Andes north of 4°N. The Panama—Choco arc may have just begun to collide with the north Andes (e.g., Coates et al., 2004; Barat et al., 2014; Montes et al., 2015).

Early-to-middle Miocene "thin-skinned" imbricate thrusting over the Garzón Massif basement rocks resulted in approximately 43 km of shortening (Saeid et al., 2017; Wolaver et al., 2015) contemporaneous with the uplift of the southern Central Cordillera (~9–16 Ma) (Villagómez and Spikings, 2013). This change in tectonic style from "thick-skinned" to "thin-skinned" deformation coincided with the northward advance of arc volcanism and "normal" Nazca subduction (Figs. 6 and 7).

Across the northern Andes, basement blocks were rapidly uplifted 7–12 km in the last 10 m.y., including the Venezuelan Andes (De Toni and Kellogg, 1993), Sierra de Perija (Shagam, 1980; Kellogg and Bonini, 1982), Santander Massif (Amaya et al., 2017), Eastern Cordillera (Fig. 5; Gregory-Wodzicki, 2000; Mora et al., 2010b; Anderson et al., 2016), Garzon Massif (Saeid et al., 2017), and the Santa Marta Massif (Villagómez et al., 2011) (For location of uplifts see Fig. 1). The spatial distribution of these numerous Laramide-style basement block uplifts correlates with buoyant Caribbean low-angle to flat slab subduction and resultant low heat flow. The timing (last 10 Myr), spatial distribution and orientation, and high rates of shortening (5–15 mm/yr) and uplift (0.5–1.0 mm/yr) also suggest that the uplifts were accelerated by the Panama-Choco—North Andes arc-continent collision and accretion, especially the Eastern Cordillera of Colombia (e.g., Kellogg and Vega, 1995; Egbue et al., 2014).

5.2 Panamá arc-North Andes collision: "broken indenter" and arc accretion

There is an apparent discrepancy between the small GPS measured margin-normal shortening in the Eastern Cordillera of Colombia and paleobotanical, radiometric, and geologic evidence for recent rapid shortening and uplift of the Cordillera. Mora-Páez et al. (2016) interpreted the small GPS measured shortening as evidence for slow formation of the Eastern Cordillera over a period of up to 40 Myr. They argue that the paleobotanical evidence for recent rapid uplift may represent local uplift or may have been influenced by climate change or invasive species from North America. Mora-Páez et al. (2019) present an alternative explanation, a "broken indenter" model for the Panamá-Choco arc collision that is consistent with the GPS data, paleobotanical, radiometric, and geologic evidence. The "broken indenter model" is also compatible with GPS evidence for the accretion of the Choco arc to the North Andes, as well as taking into account the collision of the Panama-Choco arc with the North Andes as a potential driver for crustal shortening and mountain building (Kellogg and Mora-Páez, 2016).

The new velocity field for northwestern South America and the southwest Caribbean presented by Mora-Páez et al. (2019) records margin-normal shortening of only 4.5 mm/yr in the Eastern Cordillera of Colombia (based on five sites; 3.7 ± 0.3 mm/yr according to Mora-Páez et al., 2016). However, paleobotanical, fission-track, seismic reflection, and well data from the range suggest rapid uplift (7 km) and shortening (120 km) in the last 10 Myr. This would imply an average rate of about 12 mm/yr for the last 10 Myr or about three times the present rate.

About 12–15 Ma the Eastern Cordillera of Colombia became a major sediment source (Gregory-Wodzicki, 2000; Mora et al., 2014), although some sediments were being supplied to the Eastern Foothills area as early as the Oligocene (Mora et al., 2010a; Saylor et al., 2012). Paleobotanical data (Fig. 6A; Wijninga, 1996; Gregory-Wodzicki, 2000) and apatite fission-track ages (Mora et al., 2008;

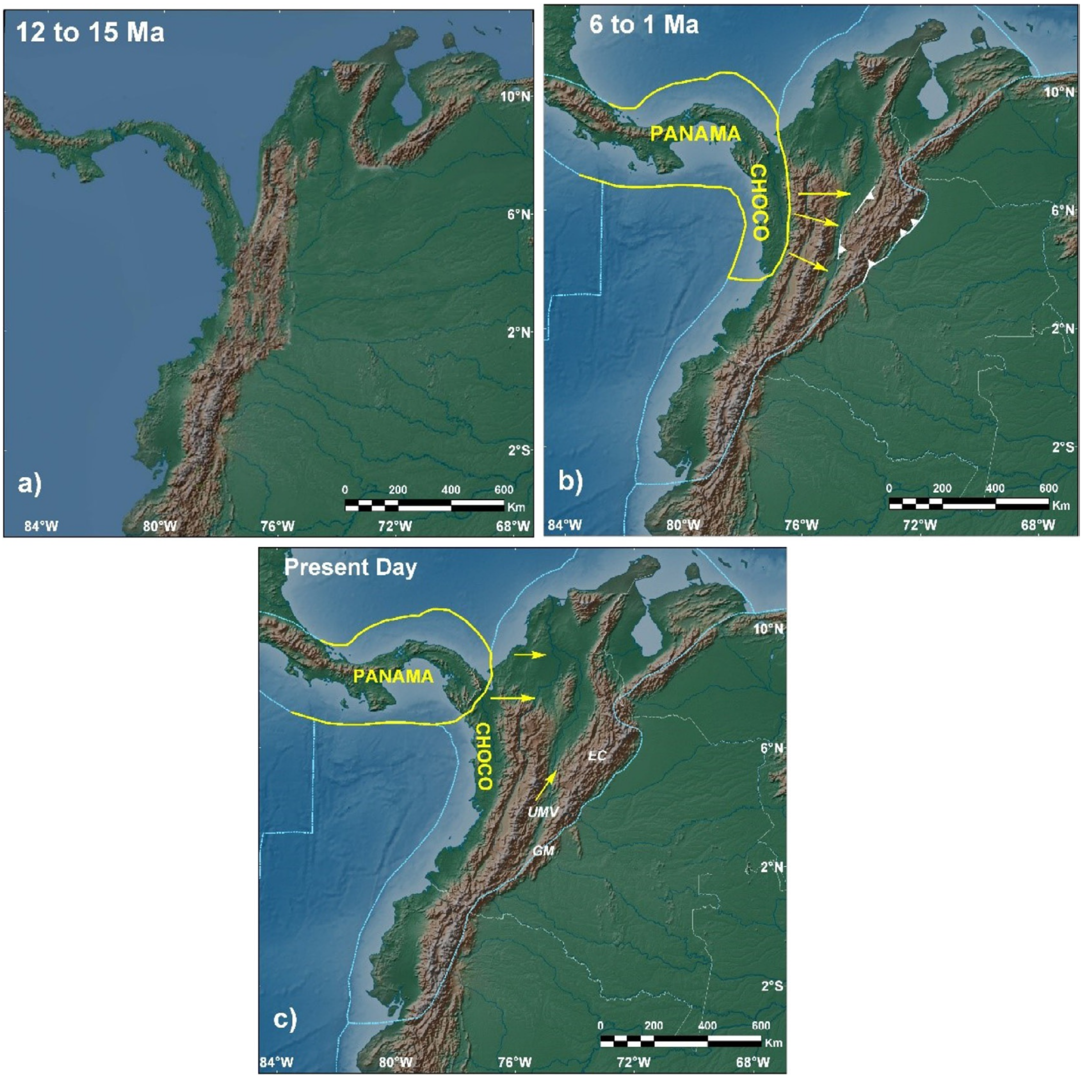

FIG. 10

Schematic evolution of Panama—North Andes after Kellogg and Mora-Páez (2016). (A) 12–15 Ma. Initial collision of Panama-Choco arc and North Andes. (B) 6–1 Ma. Panama-Choco N Andes collision. Permanent shortening and rapid uplift of *E. cordillera*. (C) Present. Choco arc is accreted to the North Andes. Upper Magdalena Valley (UMV), Eastern Cordillera (EC), Garzón Massif (GM).

Mora et al., 2010b) indicate that most of the uplift in the central and eastern flank of the Eastern Cordillera occurred in the last 12 Myr. Paleoprecipitation data from the Upper Magdalena Valley indicate that a substantial orographic barrier was not fully established until 6–3 Ma, when >1 km/m.y. of material was exhumed (Anderson et al., 2016). Based on minimum exhumational ages provided by new apatite FTA data, as well as thermal history modeling, Anderson et al. (2016) suggest that thrust-induced rapid exhumation of the Garzón Massif and southern Eastern Cordillera was focused between 6.4 and 3 Ma. Tectonic uplift for the last 12 Myr was estimated by Mora-Páez et al. (2019) and Egbue and Kellogg (2012) from present-day total structural relief and paleoelevation data. The Neogene exhumation history from apatite fission track data and low-T thermochronology (Mora et al., 2008; Parra et al., 2009) supports the rapid tectonic uplift proposed for the last 6 Myr. Using apatite fission-track data, Mora et al. (2010a) estimated exhumation rates of 1–1.5 mm/yr for compressional structures in the eastern foothills of the Eastern Cordillera over the last 3 Myr. Wittmann et al. (2011) used cosmogenic nuclide-based measurements to estimate denudation rates of 0.49–1.2 mm/yr for the Ecuadorian Andes.

Egbue and Kellogg (2012) estimated the shortening rates for the Eastern Cordillera for the last 12 Myr from the tectonic uplift rates. Shortening rates were assumed to be proportional to tectonic uplift rates and were estimated for a range of shortening models (60–120 km for the last 12 Myr) after Dengo and Covey, 1993, Cooper et al., 1995; Fig. 5, Kellogg et al., 2005a; Egbue and Kellogg, 2012; Teixell et al., 2015, yielding maximum shortening rates of 10–20 mm/a, or 2–5 times greater than the present observed rate. Range-parallel shear "escape" has become a significant factor in the last 2 Myr, and range-normal shortening rates have apparently declined abruptly.

The apparent dichotomy of rapid Miocene shortening in the Eastern Cordillera and very slow range normal shortening at present can be explained by a "broken indenter" model (Fig. 10). The rigid Panama-Choco collision with the North Andes (15-18 mm/yr at present) produced rapid permanent deformation in the North Andes, especially after the closure of the Central American Seaway and formation of the land bridge in the last 10 Myr (Fig. 10B). The present-day GPS vectors at BASO and TONE (Fig. 2), however, suggest that the Choco block is no longer part of the rigid Panama indenter but has been accreted to the NAB (Fig. 10C). If this interpretation is correct, the break in the Panama-Choco indenter and Choco accretion to the NAB must have occurred very recently (in the last 1–2 Myr) to explain the rapid Late Miocene shortening and uplift.

5.3 Bucaramanga slab—Nazca or Caribbean?

The lack of a volcanic arc over the subducting Caribbean slab for the last 50 Myr suggests that the Caribbean lithosphere may have been buoyant and subducting at a low angle under the northern Andes for over 50 Myr.

The shallow dipping "Bucaramanga slab" north of 5.5°N (Fig. 9) has been interpreted as either recently flattened Nazca lithosphere (Corredor, 2003; Zarifi et al., 2007; Sanchez-Rojas and Palma, 2014; Chiarabba et al., 2015; Syracuse et al., 2016; Wagner et al., 2017) or lithosphere of Caribbean origin (Malavé and Suárez, 1995; Taboada et al., 2000; Cortés and Angelier, 2005; Vargas et al., 2007; Prieto et al., 2012; Yarce et al., 2014). The first model interprets the 250-km offset in Wadati-Benioff zone seismicity as the Caldas "Tear" (CT) in the Nazca plate with "normal" subduction to the south and flat-slab subduction to the north (Fig. 9). The second model interprets the 250-km CT offset in seismicity as the southern boundary of the flat-subducting Caribbean plate overlying the steeper dipping Nazca slab.

Syracuse et al. (2016) presented tomographic results that they proposed were most consistent with synthetic velocity models for two nonoverlapping slabs. Wagner et al. (2017) mapped the volcanic arc activity in Colombia from 14 Ma to present and noted that regular arc volcanism extended along Colombia's entire Pacific margin in the mid-Miocene, with modern arc volcanism resuming only south of 5.5°N and after 4 Ma. Wagner et al. (2017) interpreted this volcanic pattern as indicating the formation of a Nazca flat slab during the latest Miocene with a 250-km wide tear at 5.5°N.

We have mapped the volcanic arc activity in the North Andes back to 100 Ma (last 50 Myr shown in Fig. 6 and Supplementary Data, Table 1 in the online version at https://doi.org/10.1016/B978-0-12-816009-1.00006-X). At the beginning of the Cenozoic ~70 Ma, the Caribbean plate extended over 1500 km along the entire western boundary of the NAB (Boschman et al., 2014). By 30 Ma, renewed volcanic activity marked the northward advance of the Farallon-Caribbean-South America triple junction as Farallon plate "normal" magmatic subduction began under the northern Andean margin up to ~2.3°N and by 20 Ma, as far as 3.6°N (Fig. 6), but all along the east flank of the Choco arc Caribbean lithosphere was still subducting under the NAB. A spike in volcanic activity in the Choco terrane and just east of the terrane from 15 to 5 Ma (Fig. 6B) marked the initial Panama-Choco-NAB collision. We agree with Wagner et al. (2017) that this volcanic activity was related to Nazca subduction. However, at this time, the newly arrived Nazca lithosphere was just beginning to underthrust the Caribbean slab. Five million years ago, volcanic activity abruptly ended north of 5.5°N as the shallow-dipping Caribbean slab formed a thermal blanket over the advancing asthenospheric wedge.

One of the greatest difficulties with the overlapping slab interpretation north of 5.5°N is the lack of a clear second Wadati-Benioff zone beneath the shallow subducting slab. However, we note that tomographic profiles (Syracuse et al., 2016) show high velocities beneath the Bucaramanga slab where we predict Nazca subduction. Coupling between the underlying more rapidly subducting Nazca slab and the slower overlying Caribbean plate might increase seismicity in the Caribbean slab, while trapped heat from the Nazca asthenospheric wedge could reduce seismicity in the underlying Nazca slab.

A strong argument in favor of a Caribbean origin for the Bucaramanga slab is the apparent continuity in the Wadati-Benioff slab geometry with the Caribbean slab to the north (Malavé and Suárez, 1995; Taboada et al., 2000; Cortés and Angelier, 2005; Vargas et al., 2007; Prieto et al., 2012; Yarce et al., 2014). The new plate model presented in this chapter further supports a Caribbean origin for the flat Bucaramanga slab, since our predicted present position for the southern limit of the 0–20 Ma subducted Caribbean slab (Figs. 8 and 9) coincides with the present southern edge of the Bucaramanga slab.

6 Summary

The Caribbean Large Igneous Province (CLIP) collided with South America at ~75 Ma, resulting in the obduction of the Western Cordillera island arc terrane over South American continental crust on a low-angle thrust fault. Following accretion, subduction polarity flipped to east dipping under the North Andes, the trench jumped west of the accreted terrane, and Caribbean lithosphere began subducting under the northern Andes. At 70 Ma, the Caribbean plate extended over 1500 km along the entire western boundary of the North Andean Block (NAB).

In the past 50 million years, the Caribbean has moved 1000 km eastward relative to the North and South American plates and approximately one-third of the Caribbean plate (1.3×10^6 km^2) has been subducted under northwestern South America in that time. The lack of a volcanic arc in the north Andes from 55 to 25 Ma suggests that the Caribbean plate was buoyant and subducting amagmatically at a low angle under South America as it is at present.

At 23 Ma, the Cocos plate split off from the Farallon plate, which was renamed the Nazca plate. Volcanic arc activity resumed in southern Colombia by 20 Ma, as the Nazca-Caribbean-South America triple junction moved northeastward up the north Andean margin. Relative plate convergence at the southern Colombia trench changed from northeastward Farallon motion to more eastward Nazca convergence.

The initial collision of the Panama-Choco arc and the North Andes occurred between 12 and 40 Ma. The Indonesian Australian Archipelago provides a model for the Panama Arc between 15 and 3 Ma that accounts for the tectonic closure, while also accounting for the marine fossil record of a closing Central American Seaway at 10–11 Ma and the delayed Great American Biotic Interchange at 4.2–3.5 Ma. A spike in age dates in the Choco terrane from 15 Ma to 5 Ma seems to bracket the initial Panama-Choco-North Andes collision. Shallow Caribbean subduction continued east of the Choco arc under the North Andes until the final arc-continent accretion. Five million years ago, volcanic activity abruptly ended again north of 5.5°N as the subducting Nazca lithosphere underthrust the shallow-dipping retreating Caribbean slab, which formed a thermal blanket over the advancing asthenospheric wedge.

The Panamá arc is rapidly colliding eastward with the North Andean block (NAB) at approximately 16–17 mm/yr, and the present deformation associated with the collision is confined to the North Andes north of 7.5°N latitude. The apparent dichotomy of rapid Miocene shortening in the Eastern Cordillera and slow range normal shortening at present (GPS results) can be explained by a "broken indenter" model. The rigid Panama-Choco collision with the North Andes (15–18 mm/yr at present) produced rapid permanent deformation in the North Andes. The present-day GPS vectors at BASO and TONE, however, suggest that the Choco block is no longer part of the rigid Panama indenter but has been accreted to the NAB. The present on-going collision poses a major earthquake hazard from the Panama border to Medellin, Colombia (SEL1, Fig. 2).

Caribbean flat slab subduction is characterized by a lack of a volcanic arc because there is no asthenospheric wedge in the overriding plate, with resultant low heat flow, and rigid thick-skinned "Laramide"-style basement tectonics. Caribbean subduction under the NAB at about 13 mm/yr poses a seismic hazard in northern Colombia. Across the northern Andes basement blocks were rapidly uplifted 7–12 km in the last 10 m.y., including the Venezuelan Andes, Sierra de Perija, Santander Massif, Eastern Cordillera, Garzon Massif, and the Santa Marta Massif. The spatial distribution of these numerous Laramide-style basement block uplifts correlates with buoyant Caribbean low angle to flat slab subduction and resultant low heat flow. The timing (last 10 Myr), spatial distribution and orientation, and high rates of shortening (5–15 mm/yr) and uplift (0.5–1.0 mm/yr) also suggest that the uplifts were accelerated by the Panama-Choco—North Andes arc-continent collision and accretion.

Continuity in the Wadati-Benioff slab geometry with the Caribbean slab to the north and the new plate model presented in this chapter support a Caribbean origin for the flat Bucaramanga slab, since our predicted present position for the southern limit of the subducted Caribbean slab coincides with the present Bucaramanga slab.

About 2 Ma, the aseismic Carnegie ridge, which was formed by the Galapagos hotspot, arrived at the Colombia-Ecuador trench and initiated the northeastward "escape" of the northern Andes. Presently, in the Eastern Cordillera, the escape rate (8.1 mm/yr dextral slip on the EAFZ) is greater than the rate of range-normal shortening (4.3 mm/yr). Therefore, northeast trending right-lateral strike-slip faulting is an increasing component of the seismic hazard for the Eastern Cordillera and the 8 million inhabitants of the city of Bogota.

The Colombia section of the Nazca-NAB trench continues to pose high risk of a great mega-subduction earthquake in southern Colombia. The 1942, 1958, 1979, and 2016 trench earthquakes have only released a fraction of the energy accumulated in the Ecuador-Colombia trench since the great 1906 earthquake. Interseismic strain is accumulating rapidly in the overriding plate at least as far north as Tumaco.

Acknowledgments

We thank Gómez-Tapias and others at the Colombian Geological Survey for the Colombian radiometric ages. Hypocenter locations were compiled from the International Seismological Center (ISC), Fundación Venezolana de Investigaciones Sismológicas (FUNVISIS), and la Red Sismológica Nacional de Colombia (RSNC). Empresa Colombiana de Petroleos (ECOPETROL) supplied aeromagnetic, gravity, seismic, and well data to constrain regional profiles (Figs. 4 and 5). Omar Pérez provided critical guidance to the second author, and Franck Audemard and Lydian Boschman provided constructive reviews. We thank the many CASA team members who helped collect GPS data in the north Andes over the last 30 years, especially the Colombian Geological Survey and the GeoRED team. This research was supported in part by the Colombian Government in a grant to the Colombian Geological Survey under the BPIN code 0043000220000 of the National Planning Department. Plate motions were modeled with the freely available software package GPlates (Boyden et al., 2011). Figures were made using Generic Mapping Tools (GMT) software (Wessel and Smith, 1991), ArcGIS software, and Adobe Illustrator. The data compiled for this paper can be found in the electronic supplementary data on Elsevier's Science Direct website.

Appendix: Supplementary material

Supplementary material related to this chapter can be found on the accompanying CD or online at https://doi.org/10.1016/B978-0-12-816009-1.00006-X.

References

Amaya, S., Zuluaga, C.A., Bernet, M., 2017. New fission-track age constraints on the exhumation of the central Santander Massif: implications for the tectonic evolution of the Northern Andes, Colombia. Lithos 282–283, 388–402.

Anderson, M., Alvarado, P., Zandt, G., Beck, S., 2007. Geometry and brittle deformation of the subducting Nazca Plate, Central Chile and Argentina. Geophys. J. Int. 171, 419–434.

Anderson, V.J., Horton, B.K., Saylor, J.E., Mora, A., Tesón, E., Breecker, D.O., Ketcham, R.A., 2016. Andean topographic growth and basement uplift in southern Colombia: implications for the evolution of the Magdalena. Geosphere 12 (4), 1235–1256. https://doi.org/10.1130/GES01294.1.

Audemard, F.A., 1993. Néotectonique, Sismotectonique et Aléa Sismique du Nord-ouest du Vénézuéla (Système de Failles d'Oca–Ancón). PhD thesis, Université Montpellier II, France. 369 pp + appendix.

Audemard, F.A., 2014. In: Schmitz, M., Audemard, F., Urbani, F. (Eds.), Active Block Tectonics in and Around the Caribbean: A Review in the Northeastern Limit of the South American Plate—Lithospheric Structures From Surface to the Mantle. first ed. Editorial Innovación Tecnológica, Facultad de Ingeniería-Universidad Central de Venezuela/FUNVISIS, pp. 29–77. (Chapter 2).

Audemard, F.E., Audemard, F.A., 2002. Structure of the Mérida Andes, Venezuela: relations with the South America–Caribbean geodynamic interaction. Tectonophysics 345, 299–327.

Audemard, F.A., Pantosi, D., Machette, D., Costa, C., Okumura, K., Cowan, D., Diederix, H., Ferrer, C., Participants of the South American field workshop on Paleoseismology, 1999. Trench investigation along the Mérida section of the Bocono´ fault (central Venezuelan Andes), Venezuela. Tectonophysics 308, 1–21.

Barat, F., de Lépinay, B.M., Sosson, M., Müller, C., Baumgartner, P.O., Baumgartner-Mora, C., 2014. Transition from the Farallon Plate subduction to the collision between South and Central America: geological evolution of the Panama Isthmus. Tectonophysics 622, 145–167. https://doi.org/10.1016/j.tecto.2014.03.008.

Barrero, D., 1977. Geology of the Central Western Cordillera, West of Buga and Roldanillo, Colombia. PhD thesis, Golden, Colorado School of Mines, p. 157.

Benítez, S., 1986. Síntesis geológica del graben de Jambeli. In: IV Congreso Ecuatoriano de Geología, Minería y Petróleo. vol. 1, pp. 137–160.

Bernal-Olaya, R., Mann, P., Vargas, C.A., 2015. Earthquake, tomographic, seismic reflection, and gravity evidence for a shallowly dipping subduction zone beneath the Caribbean margin of northwestern Colombia. In: Bartolini, C., Mann, P. (Eds.), Petroleum Geology and Potential of the Colombian Caribbean Margin. vol. 108. AAPG Memoir, pp. 247–270. ISBN 13: 978-0-89181-388-0.

Bezada, M.J., Levander, A., Schmandt, B., 2010. Subduction in the southern Caribbean: images from finite-frequency P wave tomography. J. Geophys. Res. 115, B12333. https://doi.org/10.1029/2010JB007682.

Boschman, L.M., van Hinsbergen, D.J.J., Torsvik, T.H., Spakman, W., Pindell, J.L., 2014. Kinematic reconstruction of the Caribbean region since the Early Jurassic. Earth Sci. Rev. 138, 102–136. https://doi.org/10.1016/j.earscirev.2014.08.007.

Bourgois, J., Calle, B., Tournon, J., Toussaint, J.-F., 1982. The Andean ophiolitic megastructures on the Buga-Buenaventura transverse (Western Cordillera-Valle Colombia). Tectonophysics 82, 207–299.

Boyden, J., Müller, R.D., Gurnis, M., Torsvik, T.H., Clark, J., Turner, M., Ivey-Law, H., Watson, R., Cannon, J., 2011. Next-generation plate-tectonic reconstructions using GPlates. In: Keller, R., Baru, C. (Eds.), Geoinformatics: Cyberinfrastruture for the Solid Earth Sciences. Cambridge University Press.

Burke, K., 1988. Tectonic evolution of the Caribbean. Annu. Rev. Earth Planet. Sci. 16, 201–230. (A88-52285 22-46). Annual Reviews, Inc., Palo Alto, CA.

Cantalamessa, G., Di Celma, C., 2004. Origin and chronology of Pleistocene marine terraces of Isla de la Plata and of flat, gently dipping surfaces of the southern coast of Cabo San Lorenzo (Manabí, Ecuador). J. S. Am. Earth Sci. 16, 633–648.

Cardozo-Puentes, A., 1988. Structural Style of the Central Western Flank of the Cordillera Oriental West of Bogota, Colombia. M.S. thesis, University of South Carolina, p. 146.

Cediel, F., Shaw, R.P., Cáceres, C., 2003. Tectonic assembly of the Northern Andean Block. In: Bartolini, C., Buffler, R.T., Blickwede, J. (Eds.), The Circum-Gulf of Mexico and the Caribbean. Hydrocarbon Habitats, Basin Formation, and Plate Tectonics, 79. AAPG Memoir, pp. 815–848.

Chiarabba, C., De Gori, P., Faccenna, C., Speranza, F., Seccia, D., Dionicio, V., Prieto, G.A., 2015. Subduction system and flat slab beneath the Eastern Cordillera of Colombia. Geochem. Geophys. Geosyst. https://doi.org/10.1002/2015GC006048.

Chlieh, M., Mothes, P., Nocquet, J.-M., Jarrin, P., Charvis, P., Cisneros, D., Font, Y., Collot, J.-Y., Villegas-Lanza, J.-C., Rolandone, F., Vallée, M., Regnier, M., Segovia, M., Martin, X., Yepes, H., 2014. Distribution of discrete seismic asperities and aseismic slip along the Ecuadorian megathrust. Earth Planet. Sci. Lett. 400, 292–301. https://doi.org/10.1016/j.epsl.2014.05.027.

Coates, A., Stallard, R., 2013. How old is the Isthmus of Panama? Bull. Mar. Sci. 89 (4), 801–813.

Coates, A.G., Collins, L.S., Aubry, M.-P., Berggren, W.A., 2004. The geology of the Darien, Panama, and the late Miocene-Pliocene collision of the Panama arc with northwestern South America. Geol. Soc. Am. Bull. 116, 1327–1344. https://doi.org/10.1130/B25275.1.

Cooper, M.A., Addison, F.T., Alvarez, R., Coral, R.M., Graham, R.H., Hayward, A.B., Howe, S., Martinez, J., Naar, J., Peñas, R., Pulham, A.J., Taborda, A., 1995. Basin development and tectonic history of the Llanos basin, Eastern Cordillera, and Middle Magdalena Valley, Colombia. AAPG Bull. 79 (10), 1421–1443.

Corredor, F., 2003. Seismic strain rates and distributed continental deformation in the northern Andes and three-dimensional seismotectonics of northwestern South America. Tectonophysics 372 (3), 147–166.

Cortés, M., Angelier, J., 2005. Current states of stress in the northern Andes as indicated by focal mechanisms of earthquakes. Tectonophysics 403 (1), 29–58.

Cross, T.A., Pilger, R.H., 1982. Controls of subduction geometry, location of magmatic arcs, and tectonics of arc and back-arc regions. Geol. Soc. Am. Bull. 93, 545–562.

De Toni, B., Kellogg, J., 1993. Seismic evidence for blind thrusting of the northwestern flank of the Venezuelan Andes. Tectonics 12, 1393–1409.

DeCelles, P.G., 2004. Late Jurassic to Eocene evolution of the Cordilleran thrust belt and foreland basin system, Western U.S.A. Am. J. Sci. 304, 105–168.

DeCelles, P.G., Ducea, M.N., Kapp, P., Zandt, G., 2009. Cyclicity in Cordilleran orogenic systems. Nat. Geosci. 2, 251–257.

DeMets, C., Gordon, R.G., Argus, D.F., 2010. Geologically current plate motions. Geophys. J. Int. 181 (1), 1–80.

Dengo, C., Covey, M., 1993. Structure of the Eastern Cordillera of Colombia: implications for trap styles and regional tectonics. AAPG Bull. 77 (8), 1315–1337.

Dewey, J.W., 1972. Seismicity and tectonics of western Venezuela. Bull. Seismol. Soc. Am. 62, 1711–1751.

Duque, H., 1994. Structural styles and hydrocarbon prospective areas in the Eastern Cordillera, Colombia. M.S. thesis, University of South Carolina.

Duque-Caro, H., 1990. The Chocó block in the northwestern corner of South America: structural, tectonostratigraphic and paleogeographic implications. J. S. Am. Earth Sci. 3, 1–14.

Egbue, O., Kellogg, J., 2010. Pleistocene to present North Andean “escape”. Tectonophysics 489, 248–257. https://doi.org/10.1016/j.tecto.2010.04.021.

Egbue, O., Kellogg, J., 2012. Three-dimensional structural evolution and kinematics of the Piedemonte Llanero, Central Llanos foothills, Eastern Cordillera, Colombia. J. S. Am. Earth Sci. https://doi.org/10.1016/j.jsames.2012.04.012.

Egbue, O., Kellogg, J., Aguirre, H., Torres, C., 2014. Evolution of the stress and strain fields in the Eastern Cordillera, Colombia. J. Struct. Geol. 58, 8–21.

Ego, F., Sebriera, M., Lavenuc, A., Yepes, H., Egues, A., 1996. Quaternary state of stress in the northern Andes and the restraining bend model for the Ecuadorian Andes. Tectonophysics 259 (1–3), 101–116.

Fan, M., Carrapa, B., 2014. Late Cretaceous-early Eocene Laramide uplift, exhumation, and basin subsidence in Wyoming: crustal responses to flat slab subduction. Tectonics 33, 509–529. https://doi.org/10.1002/2012TC003221.

Franco, G.B., 2017. Evolución geofísica y tectónica de los Andes Septentrionales. Thesis, Universidad Simón Bolívar, Caracas, p. 118.

Freymueller, J.T., Kellogg, J.N., Vega, V., 1993. Plate motions in the north Andean region. J. Geophys. Res. 98, 21853–21863.

FUNVISIS, 2017. Venezuelan Foundation for Seismological Research, Earthquake Catalogs. http://www.funvisis.gob.ve/.

Gómez-Tapias, N., Montes-Ramírez, F., Alcárcel-Gutiérrez, A., Ceballos-Hernández, J.A., 2013. Catálogo de Dataciones Radiométricas De Colombia En ArcGis 9.3 y Google Earth. Servicio Geológico Colombiano, Bogotá.

Gregory-Wodzicki, K.M., 2000. Andean paleoelevation estimates: a review and critique. GSA Bull. 112, 1091–1105.

Gutscher, M.A., Olivet, J.L., Aslanian, D., Eissen, J.P., Maury, R., 1999. The “lost Inca Plateau”: cause of flat subduction beneath Peru? Earth Planet. Sci. Lett. 171, 335–341.

Gutscher, M.A., Spakman, W., Bijwaard, H., Engdahl, E.R., 2000. Geodynamics of flat subduction: seismicity and tomographic constraints from the Andean margin. Tectonics 19, 814–833.

Horton, B.K., 2018. Sedimentary record of Andean mountain building. Earth Sci. Rev. 178, 279–309. https://doi.org/10.1016/j.earscirev.2017.11.025.

ISC, 2013. Bulletin of the International Seismological Centre. International Seismological Centre, Thatcham. online: http://www.isc.ac.uk.

James, D.E., Sacks, I.S., 1999. Cenozoic Formation of the Central Andes: A Geophysical Perspective. vol. 7 Society of Economic Geologists (Special Publication). US 1–25.

Jordan, T.E., Allmendinger, R.W., 1986. The Sierras Pampeanas of Argentina: a modern analogue of Rocky mountain foreland deformation. Am. J. Sci. 286, 737–764. https://doi.org/10.2475/ajs.286.10.737.

Jordan, T., Isacks, B., Allmendinger, R., Brewer, J., Ramos, V., Ando, C., 1983. Andean tectonics related to geometry of the subducted Nazca plate. Geol. Soc. Am. Bull. 94, 341–361.

Keigwin, L.D., 1978. Pleistocene closing of the Isthmus of Panama, based on biostratigraphic evidence from nearby Pacific Ocean and Caribbean Sea cores. Geology 6, 630–634.
Kellogg, J.N., 1984. The Cenozoic tectonic history of the Sierra de Perija and adjacent basins. In: Bonini, W.E., Hargraves, R.B., Shagam, R. (Eds.), Caribbean—South American Plate Boundary and Regional Tectonics. Memoirs—Geological Society of America, vol. 162, pp. 239–261.
Kellogg, J.N., Bonini, W.E., 1982. Subduction of the Caribbean Plate and basement uplifts in the overriding South America plate. Tectonics 1 (3), 251–276.
Kellogg, J., Mora-Páez, H., 2016. Panama Arc-North Andes Collision: "Broken Indenter" Model From New GPS Velocity Field, IASPEI—Regional Assembly. Latin-American and Caribbean Seismological Commission—LACSC, San José.
Kellogg, J., Vega, V., 1995. Tectonic development of Panama, Costa Rica, and the Colombian Andes: constraints from Global Positioning System geodesy studies and gravity. In: Mann, P. (Ed.), Geologic and Tectonics Development of the Caribbean Plate Boundary in Southern Central America. Geological Society of America, Boulder, CO. Special Paper 295.
Kellogg, J.N., Freymueller, J.T., Dixon, T.H., Neilan, R.E., Ropain, U., Camargo, M., Fernandez, C., Stowell, J.L., Salazar, A., Jaime, M.V., Espin, L., Perdue, V., Leos, L., 1990. First GPS baseline results from the North Andes, CASA UNO Special Issue. Geophys. Res. Lett. 17, 211–214.
Kellogg, J., Ojeda, G., Duque, H., Ceron, J., 2005a. Crustal structure of the Eastern Cordillera, Colombia. In: 6th International Symposium on Andean Geodynamics, Barcelona, pp. 424–427.
Kellogg, J., Toto, E., Ceron, J., 2005b. Structure and tectonics of the Sinu-San Jacinto accretionary prism in northern Colombia. In: X Congreso Colombiano de Geología, Bogota. 10 pp.
Kennan, L., Pindell, J., 2009. Dextral shear, terrane accretion and basin formation in the Northern Andes: best explained by interaction with a Pacific-derived Caribbean Plate? Geol. Soc. Lond. Spec. Publ. 328, 487–531.
Kerr, A.C., Tarney, J., 2005. Tectonic evolution of the Caribbean and northwestern South America: the case for accretion of two Late Cretaceous oceanic plateaus. Geology 33, 269–272.
Kerr, A.C., Marriner, G.F., Tarney, J., Nivia, A., Saunders, A.D., Thirlwall, M.F., Sinton, C.W., 1997. Cretaceous basaltic terranes in Western Colombia: elemental, chronological and Sr-Nd isotopic constraints on petrogenesis. J. Petrol. 38, 677–702.
Klitgord, K.D., Schouten, H., 1986. Plate kinematics of the Central Atlantic. In: Vogt, P.R., Tucholke, B.E. (Eds.), The Geology of North America. Vol. M. The Western North Atlantic Region (A Decade of North American Geology). Geological Society of America, Boulder, CO. (Chapter 22, 50 pp.).
Kobayashi, D., LaFemina, P., Geirsson, H., Chichaco, E., Abrego, A., Mora-Páez, H., Camacho, E., 2014. Kinematics of the western Caribbean collision of the Cocos Ridge and upper plate deformation. Geochem. Geophys. Geosyst. 1671–1683. https://doi.org/10.1002/2014GC005234.
Ladd, J.W., Truchan, M., Talwani, M., Stoffa, P.L., Buhl, P., Houtz, R., Mauffret, A., Westbrook, G.K., 1984. Seismic reflection profiles across the southern margin of the Caribbean. In: Bonini, W.E., Hargraves, R.B., Shagam, R. (Eds.), The Caribbean-South American Plate Boundary and Regional Tectonics. Memoir—Geological Society of America, pp. 153–159.
León, S., Cardona, A., Parra, M., Sobel, E.R., Jaramillo, J.S., Glodny, J., Pardo-Trujillo, A., 2018. Transition from collisional to subduction-related regimes: an example from Neogene Panama-Nazca-South America interactions. Tectonics 37, https://doi.org/10.1002/2017TC004785.
Leroy, S., Mauffret, A., Patriat, P., Mercier de Lépinay, B., 2000. An alternative interpretation of the Cayman trough evolution from a reidentification of magnetic anomalies. Geophys. J. Int. 141, 539–557.
Lissinna, B., 2005. A profile through the Central American Landbridge in western Panama: 115 Ma Interplay between the Galápagos Hotspot and the Central American Subduction Zone. Ph. D. Thesis, Christian Albrechts-Universität zu Kiel. 102 p.
Liu, L., Spasojevi, S., Gurnis, M., 2008. Reconstructing Farallon plate subduction beneath North America back to the late cretaceous. Science 322, 934–938.

Liu, L., Gurnis, M., Seton, M., Saleeby, J., Muller, R.D., Jackson, J.M., 2010. The role of oceanic plateau subduction in the Laramide orogeny. Nat. Geosci. 3, 353–357.

Livaccari, R.F., Burke, K., Sengor, A.M.C., 1981. Was the Laramide orogeny related to subduction of an oceanic plateau? Nature 289, 276–278.

Lonsdale, P., 2005. Creation of the Cocos and Nazca plates by fission of the Farallon plate. Tectonophysics 404 (3-4), 237–264. https://doi.org/10.1016/j.tecto.2005.05.011.

Lonsdale, P., Klitgord, K.D., 1978. Structure and tectonic history of the eastern Panama Basin. GSA Bull. 89, 981–999.

Malavé, G., Suárez, G., 1995. Intermediate-depth seismicity in northern Colombia and western Venezuela and its relationship to Caribbean plate subduction. Tectonics 14 (3), 617–628.

McCaffrey, R., 1996. Estimates of modern arc-parallel strain rates in fore arcs. Geology 24, 27–30.

McCaffrey, R., 2002. Crustal block rotations and plate coupling. In: Stein, S., Freymueller, J. (Eds.), Plate Boundary Zones. AGU Geodynamics Series, 30, pp. 101–122.

McCourt, W.J., Aspden, J.A., Brook, M., 1984. New geological and geochronological data from the Colombian Andes: continental growth by multiple accretion. J. Geol. Soc. Lond. 141, 831–845.

Meissner, R.O., Flueh, E.R., Stibane, F., Berg, E., 1976. Dynamics of the active plate boundary in southwest Colombia according to recent geophysical measurements. Tectonophysics 35, 115–136.

Meschede, M., Frisch, W., 1998. A plate-tectonic model for the Mesozoic and Early Cenozoic history of the Caribbean plate. Tectonophysics 296, 269–291.

Miller, J., Mitra, S., 2011. Deformation and secondary faulting associated with basement-involved compressional and extensional structures. AAPG Bull. 95, 675–689.

Montes, C., Bayona, G., Cardona, A., Buchs, D.M., Silva, C.A., Morón, S., Hoyos, N., Ramírez, D.A., Jaramillo, C.A., Valencia, V., 2012. Arc-continent collision and orocline formation: closing of the Central American seaway. J. Geophys. Res. 117, B04105. https://doi.org/10.1029/2011JB008959.

Montes, C., Cardona, A., Jaramillo, C., Pardo, A., Silva, J.C., Valencia, V., Ayala, C., Perez-Angel, L.C., Rodriguez-Parra, L.A., Ramirez, V., Nino, H., 2015. Middle Miocene closure of the Central American Seaway. Science 348 (6231), 226–229.

Mora, A., Parra, M., Strecker, M.R., Sobel, E.R., Hooghiemstra, H., Torres, V., Vallejo, J.J., 2008. Climatic forcing of asymmetric orogenic evolution in the Eastern Cordillera of Colombia. GSA Bull. 120 (7/8), 930–949.

Mora, A., Horton, B.K., Mesa, A., Rubiano, J., Ketcham, R.A., Parra, M., Blanco, V., Garcia, D., Stockli, D.F., 2010a. Migration of Cenozoic deformation in the Eastern Cordillera of Colombia interpreted from fission track results and structural relationships: implications for petroleum systems. AAPG Bull. 94 (10), 1543–1580. https://doi.org/10.1306/01051009111.

Mora, A., Parra, M., Strecker, M.R., Sobel, E.R., Zeilinger, G., Jaramillo, C., Da Silva, S., Blanco, M., 2010b. The eastern foothills of the Eastern Cordillera of Colombia: an example of multiple factors controlling structural styles and active tectonics. Geol. Soc. Am. Bull. 112, 1846–1864. https://doi.org/10.1130/B30033.1.

Mora, A., Ketcham, R.A., Higuera-Diaz, I.C., Bookhagen, B., Jimenez, L., Rubiano, J., 2014. Formation of passive-roof duplexes in the Colombian Subandes and Peru. Lithosphere 6 (6), 456–472.

Mora, J.A., Oncken, O., Le Breton, E., Mora, A., Veloza, G., Vélez, V., de Freitas, M., 2018. Controls on forearc basin formation and evolution: insights from Oligocene to Recent tectono-stratigraphy of the Lower Magdalena Valley basin of northwest Colombia. Mar. Pet. Geol. 97, 288–310. https://doi.org/10.1016/j.marpetgeo.2018.06.032.

Mora-Páez, H., 1995. Central and South America GPS geodesy: relative plate motions determined from 1991 and 1994 measurements in Colombia, Costa Rica, Ecuador, Panama and Venezuela. M.S. Thesis, University of South Carolina, Columbia, p. 94.

Mora-Páez, H., Mencin, D.J., Molnar, P., Diederix, H., Cardona-Piedrahita, L., Juan-Ramón, P.-G., Corchuelo-Cuervo, Y., 2016. GPS velocities and the construction of the Eastern Cordillera of the Colombian Andes. Geophys. Res. Lett. 43, 8407–8416. https://doi.org/10.1002/2016GL069795.

Mora-Paez, H., Kellogg, J., Freymueller, J., Mencin, D., Fernandes, R.M., Diederix, H., LaFemina, P., Cardona-Piedrahita, L., Lizarazo, S., Pelaez-Gaviria, J.R., Díaz-Mila, F., Bohorquez-Orozco, O.P., Giraldo-Londoño, L., Corchuelo-Cuervo, Y., 2019. Crustal deformation in the northern Andes – Space geodesy velocity field. J. South Am. Earth Sci. 89, 76–91. https://doi.org/10.1016/j.jsames.2018.11.002.

Müller, R.D., Royer, J.-Y., Cande, S.C., Roest, W.R., Maschenkov, S., 1999. New constraints on the Late Cretaceous/Tertiary plate tectonic evolution of the Caribbean. In: Mann, P. (Ed.), Caribbean Basins. Elsevier Science B.V, Amsterdam, pp. 33–59.

Namson, J., Cunningham, R., Woodcock, G., 1994. Structural geology and hydrocarbon potential of the northern part of the Upper Magdalena Basin, Colombia. In: V Simposio Bolivariano Exploracion Petrolera en las Cuencas Subandinas, Puerto La Cruz, Venezuela, pp. 356–364.

Nocquet, J., Villegas-Lanza, J.C., Chlieh, M., Mothes, P.A., Rolandone, F., Jarrin, P., Cisneros, D., Alvarado, A., Audin, L., Bondoux, F., Martin, X., Font, Y., Régier, M., Vallée, M., Tran, T., Beauval, C., Maguiña Mendoza, J.M., Martinez, W., Tavera, H., Yepes, H., 2014. Motion of continental slivers and creeping subduction in the Northern Andes. Nat. Geosci. 7 (4), 287–291. https://doi.org/10.1038/NGEO2099.

Nocquet, J.-M., Jarrin, P., Vallée, M., Mothes, P.A., Grandin, R., Rolandone, F., Delouis, B., Yepes, H., Font, Y., Fuentes, D., Régnier, M., Laurendeau, A., Cisneros, D., Hernandez, S., Sladen, A., Singaucho, J.-C., Mora-Páez, H., Gomez, J., Monte, L., Charvis, P., 2017. Supercycle at the Ecuadorian subduction zone revealed after the 2016 Pedernales earthquake. Nat. Geosci. 10, 145–149. https://doi.org/10.1038/ngeo2864.

Nur, A., Ben-Avraham, Z., 1983. Volcanic gaps due to oblique consumption of aseismic ridges. Tectonophysics 99, 355–362.

Ojeda, A., Havskov, J., 2001. Crustal structure and local seismicity in Colombia. J. Seismol. 649 (4), 575–593.

Parra, M., Mora, A., Sobel, E.R., Strecker, M.R., González, R., 2009. Episodic orogenic-front migration in the northern Andes: constraints from low-temperature thermochronology in the Eastern Cordillera, Colombia. Tectonics 28, TC4004. https://doi.org/10.1029/2008TC002423.

Pedoja, K., 2003. Les terrasses marines de la marge Nord Andine (Equateur et Nord Pe'rou): Relations avec le contexte ge'odynamique. Ph.D. thesis, University of Paris VI, Paris. 413 p.

Pennington, W.D., 1981. Subduction of the eastern Panama Basin and seismotectonics of northwestern South America. J. Geophys. Res. 86 (B11), 10753–10770.

Pérez, O.J., Wesnousky, S.G., De La Rosa, R., Marquez, J., Uzcátegui, R., Quintero, C., Liberal, L., Mora-Páez, H., Szeliga, W., 2018. On the interaction of the North Andes plate with the Caribbean and South American plates in northwestern South America from GPS geodesy and seismic data. Geophys. J. Int. 214 (3), 1986–2001. https://academic.oup.com/gji/article/214/3/1986/5035819.

Pilger, R.H., 1981. Plate reconstructions, aseismic ridges, and low-angle subduction beneath the Andes. Geol. Soc. Am. Bull. 92, 448–456.

Pindell, J.L., Barrett, S.F., 1990. Geological evolution of the Caribbean region: a plate tectonic perspective. In: Dengo, G., Case, J.E. (Eds.), The Caribbean Region: The Geology of North America. H. Geological Society of America, Boulder, CO, pp. 405–432.

Pindell, J.L., Kennan, L., 2009. Tectonic evolution of the Gulf of Mexico, Caribbean and northern South America in the mantle reference frame: an update. In: James, K.H., Lorente, M.A., Pindell, J.L. (Eds.), The Origin and Evolution of the Caribbean plate. Geological Society, London, pp. 1–55. Special Publications. 328.

Pindell, J.L., Cande, S.C., Pitman, W.C., Rowley, D.B., Dewey, J.F., Labrecque, J., Haxby, W., 1988. A plate-kinematic framework for models of Caribbean evolution. Tectonophysics, 121–138.

Prieto, G.A., Beroza, G.C., Barrett, S.A., López, G.A., Florez, M., 2012. Earthquake nests as natural laboratories for the study of intermediate-depth earthquake mechanics. Tectonophysics 570, 42–56.

Ramos, V.A., Folguera, A., 2009. Andean Flat-Slab Subduction Through Time. Geological Society, London, pp. 31–54. (Special Publications), 327.

Ramos, V.A., Cristallini, E.O., Pérez, D.J., 2002. The pampean flat-slab of the central Andes. J. S. Am. Earth Sci. 15, 59–78. https://doi.org/10.1016/S0895-9811(02)00006-8.

Rosencrantz, E., Sclater, J.G., 1986. Depth and age in the Cayman Trough. Earth Planet. Sci. Lett. 79, 133–144.

Rosencrantz, E., Ross, M., Sclater, J., 1988. Age and spreading history of the Cayman trough as determined from depth, heat flow, and magnetic anomalies. J. Geophys. Res. 93, 2141–2157.

Ross, M., Scotese, C., 1988. A hierarchical tectonic model of the Gulf of Mexico and Caribbean region. Tectonophysics 155, 139–168.

Roy, A., 1988. Evolution of the Igneous Activity in Southeastern Costa Rica and Southwestern Panama From the Middle Tertiary to the Recent. Geological Sciences, Lousianna State University, Baton Rouge, LA, p. 301.

RSNC, 2017. Catálogo Sismológico Colombiano. Red Sismológica Nacional de Colombia. http://200.119.88.135/RSNC/index.php/consultas/consulexp.

Saeid, E., Bakioglu, K.B., Kellogg, J., Leier, A., Martinez, J.A., Guerrero, E., 2017. Garzón Massif basement tectonics: structural control on evolution of petroleum systems in Upper Magdalena and Putumayo basins, Colombia. Mar. Pet. Geol. 88, 381–401. https://doi.org/10.1016/j.marpetgeo.2017.08.035.

Saleeby, J., 2003. Segmentation of the Laramide slab—evidence from the southern Sierra Nevada region. Geol. Soc. Am. Bull. 115, 665–668.

Sanchez-Rojas, J., Palma, M., 2014. Crustal density structure in northwestern South America derived from analysis and 3-D modeling of gravity and seismicity data. Tectonophysics 634, 97–115. https://doi.org/10.1016/j.tecto.2014.026.

Saylor, J., Horton, B., Stockli, D., Mora, A., Corredor, J., 2012. Structural and thermochronological evidence for Paleogene basement-involved shortening in the axial Eastern Cordillera, Colombia. J. S. Am. Earth Sci. 39, 202–215.

Schubert, C., Henneberg, H., 1975. Geological and geodetic investigations on the movement along the Bocono´ fault, Venezuelan Andes. Tectonophysics 29, 199–207.

Shagam, R., 1980. Fission track ages on apatite, zircon and sphene from rocks of the Andes, Perijá and Toas island: Venezuela. Dirección de Geología, Ministerio de Energía y Minas. Internal Report no. 9, 35 p.

Silver, E.A., Case, J.E., MacGillavry, H.J., 1975. Geophysical study of the Venezuelan borderland. Geol. Soc. Am. Bull. 86, 213–226.

Smithson, S.B., Brewer, J., Kaufman, S., Oliver, J., Hurich, C., 1978. Nature of the Wind River thrust, Wyoming, from COCORP deep-reflection data and from gravity data. Geology 6, 648–652.

Spikings, R., Cochrane, R., Villagomez, D., Van der Lelij, R., Vallejo, C., Winkler, W., Beate, B., 2015. The geological history of northwestern South America: from Pangaea to the early collision of the Caribbean Large Igneous Province (290–75 Ma). Gondwana Res. 27, 95–139. https://doi.org/10.1016/j.gr.2014.06.004.

Symithe, S., Calais, E., de Chabalier, J.B., Robertson, R., Higgins, M., 2015. Current block motions and strain accumulation on active faults in the Caribbean. J. Geophys. Res. Solid Earth 120, 3748–3774. https://doi.org/10.1002/2014JB011779.

Syracuse, E.M., Maceira, M., Prieto, G.A., Zhang, H., Ammon, C.J., 2016. Multiple plates subducting beneath Colombia, as illuminated by seismicity and velocity from the joint inversion of seismic and gravity data. Earth Planet. Sci. Lett. 444, 139–149.

Taboada, A., Rivera, L.A., Fuenzalida, A., Cisternas, A., Philip, H., Bijwaard, H., Rivera, C., 2000. Geodynamics of the northern Andes: subductions and intracontinental deformation (Colombia). Tectonics 19 (5), 787–813.

Teixell, A., Teson, E., Ruiz, J.C., Mora, A., 2015. The structure of an inverted back-arc rift: insights from a transect across the Eastern Cordillera of Colombia near Bogota. In: Bartolini, C., Mann, P. (Eds.), Petroleum Geology and Potential of the Colombian Caribbean Margin. 108. AAPG Memoir, pp. 499–516.

Tibaldi, A., Rovida, A., Corazzato, C., 2007. Late quaternary kinematics, slip-rate and segmentation of a major Cordillera-parallel transcurrent fault: the Cayambe-Afiladores-Sibundoy system, NW South America. J. Struct. Geol. 29, 664–680.

Toto, E., 1991. Geophysical structural study of the North Colombia fold belt—an active accretionary wedge. PhD Dissertation, University of South Carolina, South Carolina. 101 p.

Tousaint, J.-F., 1978. Grandes Rasgos Geológicos de la Parte Septentrional Del Occidente Colombiano. vol. 3 Universidad Nacional de Colombia, Boletin de Ciencias de la Tierra, Medellín, p. 231.

Trenkamp, R., Kellogg, J.N., Freymuller, J.T., Mora-Páez, H.P., 2002. Wide plate margin deformation, South Central America and Northwestern South America, CASA GPS observations. J. S. Am. Earth Sci. 15, 157–171.

Vallée, M., Nocquet, J.-M., Battaglia, J., Font, Y., Segovia, M., Réhnier, M., Mothes, P., Jarrin, P., Cisneros, D., Vaca, S., Yepes, H., Martin, X., Béthoux, N., Chlieh, M., 2013. Intense interface seismicity triggered by a shallow slip event in the Central Ecuador subduction zone. J. Geophys. Res. Solid Earth 118, 2965–2981. https://doi.org/10.1002/jgrb.50216.

Vallejo, C., Spikings, R.A., Luzieux, L., Winkler, W., Chew, D., Page, L., 2006. The early interaction between the Caribbean Plateau and the NW South American Plate. Terra Nova 18, 264–269.

van Benthem, S.A.C., Govers, R., 2010. The Caribbean plate: pulled, pushed, or dragged? J. Geophys. Res. 115, B10409. https://doi.org/10.1029/2009JB006950.

van Benthem, S.A.C., Govers, R., Spakman, W., Wortel, M.J.R., 2013. Tectonic evolution and the mantle structure under the Caribbean region. J. Geophys. Res. Solid Earth 118, 3019–3036. https://doi.org/10.1002/jgrb.50235.

van der Hilst, R., Mann, P., 1994. Tectonic implications of tomographic images of subducted lithosphere beneath northwestern South America. Geology (Boulder) 22, 451–454.

van der Meer, D.G., Spakman, W., Van Hinsbergen, D.J.J., Amaru, M.K., Torsvik, T.H., 2010. Towards absolute plate motions constrained by lower-mantle slab remnants. Nat. Geosci. 3, 36–40.

van Hunen, J., van den Berg, A.P., Vlaar, N.J., 2004. Various mechanisms to induce present-day shallow flat subduction and implications for the younger Earth: a numerical parameter study. Phys. Earth Planet. Inter. 146, 179–194.

Vargas, C.A., Mann, P., 2013. Tearing and breaking off of subducted slabs as the result of collision of the Panama Arc-Indenter with northwestern South America. Bull. Seismol. Soc. Am. 103 (3), 2025–2046. https://doi.org/10.1785/0120120328.

Vargas, C.A., Pujades, L.G., Montes, L.A., 2007. Seismic structure of south-central Andes of Colombia by tomographic inversion. Geofísc. Dermatol. Int. 46 (2), 117–127.

Villagómez, D., Spikings, R., 2013. Thermochronology and tectonics of the central and western cordilleras of Colombia: early cretaceous-tertiary evolution of the northern Andes. Lithos 160–161, 228–249.

Villagómez, D., Spikings, R., Mora, A., Guzmán, G., Ojeda, G., Cortés, E., Van der Lelij, R., 2011. Vertical tectonics at a continental crust-oceanic plateau plate boundary zone: fission track thermochronology of the Sierra Nevada de Santa Marta, Colombia. Tectonics 30, https://doi.org/10.1029/2010TC002835.

Wagner, L.S., Jaramillo, J.S., Ramirez-Hoyos, L.F., Monsalve, G., Cardona, A., Becker, T.W., 2017. Transient slab flattening beneath Colombia. Geophys. Res. Lett. 44, 6616–6623. https://doi.org/10.1002/2017GL073981.

Wallace, T.C., Beck, S.L., 1993. The Oct. 17-18, 1992 Colombian earthquakes; slip partitioning or faulting complexity. Seismol. Res. Lett. 64, 29–35.

Wegner, W., Wörner, G., Harmon, R.S., Jicha, B.R., 2011. Magmatic history and evolution of the Central American Land Bridge in Panama since Cretaceous times. Geol. Soc. Am. Bull. 123 (3–4), 703–724. https://doi.org/10.1130/b30109.1.

Wessel, P., Smith, W.H.F., 1991. Free software helps map and display data. EOS Trans. 72, 441–448.

White, S.M., Trenkamp, R., Kellogg, J.N., 2003. Recent crustal deformation and the earthquake cycle along Ecuador-Colombia subduction zone. Earth Planet. Sci. Lett. 216, 231–242.

Wijninga, V.M., 1996. Neogene ecology of the Salto de Tequendama site (2475 m altitude, Cordillera Oriental, Colombia): the paleobotanical record of montane and lowland forests. Rev. Palaeobot. Palynol. 92, 97–156.

Wittmann, H., von Blanckenburg, F., Guyot, J.L., Laraque, A., Bernal, C., Kubik, P.W., 2011. Sediment production and transport from in situ-produced cosmogenic 10Be and river loads in the Napo River basin, an upper Amazon tributary of Ecuador and Peru. J. S. Am. Earth Sci. 31 (1), 45–53. https://doi.org/10.1016/j.jsames.2010.09.004.

Wolaver, B.D., Coogan, J.C., Horton, B.K., Suarez Bermudez, L., Sun, A.Y., Wawrzyniec, T.F., Zhang, T., Shanahan, T.M., Dunlap, D.B., Costley, R.A., de la Rocha, L., 2015. Structural and hydrogeologic evolution of the Putumayo basin and adjacent fold-thrust belt, Colombia. Am. Assoc. Pet. Geol. Bull. 99, 1893–1927. https://doi.org/10.1306/05121514186.

Woodward, N.B., Boyer, S.E., Suppe, J., 1989. Balanced Geological Cross-Sections: An Essential Technique in Geological Research and Exploration, Short Course in Geology. vol. 6 American Geophysical Union, Washington, DC. 132 p.

Yarce, Y., Monsalve, G., Becker, T.W., Cardona, A., Poveda, E., Alvira, D., Ordoñez-Carmona, O., 2014. Seismological observations in Northwestern South America: evidence for two subduction segments, contrasting crustal thicknesses and upper mantle flow. Tectonophysics 637, 57–67.

Ye, L., Kanamori, H., Avouac, J.P., Li, L., Cheung, K.F., Lay, T., 2016. The 16 April 2016, Mw 7.8 (Ms 7.5) Ecuador earthquake: a quasi-repeat of the 1942 Ms 7.5 earthquake and partial re-rupture of the 1906 Ms 8.6 Colombia-Ecuador earthquake. Earth Planet. Sci. Lett. 454, 248–258. https://doi.org/10.1016/j.epsl.2016.09.006.

Zarifi, Z., Havskov, J., Hanyga, A., 2007. An insight into the Bucaramanga nest. Tectonophysics 443 (1), 93–105.